이학석사 학위논문

Lapatinib에 대한 획득 내성을 지닌 HER2 양성 유방암 세포주에서 CDK4/6 억제제인 palbociclib의 항종양효과 및 작용 기전에 관한 연구

Antitumor effect of CDK4/6 inhibitor, palbociclib, in acquired lapatinib resistant HER2-positive breast cancer cells

2019년 8월

서울대학교 대학원

협동과정 종양생물학 전공

정 다 은

이학석사 학위논문

Lapatinib에 대한 획득 내성을 지닌 HER2 양성 유방암 세포주에서 CDK4/6 억제제인 palbociclib의 항종양효과 및 작용 기전에 관한 연구

Antitumor effect of CDK4/6 inhibitor, palbociclib, in acquired lapatinib resistant HER2-positive breast cancer cells

2019년 8월

서울대학교 대학원

협동과정 종양생물학 전공

정 다 은

Lapatinib에 대한 획득 내성을 지닌 HER2 양성 유방암 세포주에서 CDK4/6 억제제인 palbociclib의 항종양효과 및 작용 기전에 관한 연구

지도교수 임석아

이 논문을 이학석사 학위논문으로 제출함

2019년 4월

서울대학교 대학원

협동과정 종양생물학 전공

정 다 은

정다은의 석사학위논문을 인준함

2019년 7월

위 원 장 _____ (인)

부 위 원 장 _____ (인)

위 원 _____ (인)

Antitumor effect of CDK4/6 inhibitor, palbociclib, in acquired lapatinib resistant HER2-positive breast cancer cells

by

Da Eun Jeong

(Directed by Seock-Ah Im, M.D., Ph.D.)

A Thesis Submitted to the Interdisciplinary Graduate Program in Partial Fulfillment of the Requirements for the Degree of Master of Science In Cancer Biology at the Seoul National University, Seoul, Korea

July, 2019

Approved by thesis committee:

Professor _____Chairperson

Professor _____Vicechairperson

Professor _____

Abstract

Antitumor effect of CDK4/6 inhibitor, palbociclib, in acquired lapatinib resistant HER2-positive breast cancer cells

Da Eun Jeong

Major in Cancer Biology

Interdisciplinary Graduate Program

The Graduate school

Seoul National University

Background: Lapatinib is a dual tyrosine kinase inhibitor which interrupts the HER2/neu and epidermal growth factor receptor (EGFR) family pathways in solid tumors. It is used for the treatment of patients with advanced or metastatic breast cancer whose tumors

overexpress HER2. Majority of patients who initially respond to the treatment will eventually progress due to acquired resistance. The defect in cell cycle regulation via increased levels of cyclin D-CDK4/6 complexes is a well-known mechanism of the acquired resistance to lapatinib. Thus, CDK4/6 inhibition can be considered as an attractive strategy to overcome lapatinib resistance. In this study, antitumor effect of palbociclib, a CDK4/6 inhibitor was investigated whether it can be used as a new strategy to treat lapatinib resistant cells by modulating cell cycle regulation.

Methods: Acquired lapatinib resistant SK-BR-3 cells are established by treating lapatinib consistently for 7 months. The characteristics of lapatinib resistance (LR) cell lines were evaluated by MTT, FACS, Western blotting, qPCR, methylation assay and transcriptome analysis. The antitumor effects of palbociclib in SK-BR-3 LR cell lines were evaluated through changes in proliferative ability using MTT and colony forming assay. Mechanism of action was analyzed by BrdU assay, β-galactosidase assay, Western blotting assay for signal

transduction molecules and IFA.

Results: In SK-BR-3 LR cells, the change of the molecules that were related to the G1/S transition of cell cycle was prominent. It was confirmed that cell cycle progression and proliferation were significantly faster in SK-BR-3 LR cells compared to parental cells. Overexpression of cyclin D1 and CDK6 was shown in SK-BR-3 LR cells but cyclin-dependent kinase inhibitor, p16 and p14 were suppressed. Cyclin D1 and CDK6 were upregulated at the transcription level, and the epigenetic suppression of *CDKN2A* was observed. Palbociclib inhibited the cell cycle progression and reduced the cell viability significantly in SK-BR-3 LR cells by cell cycle arrest via blocking hyper-phosphorylation of Rb. Palbociclib also induced autophagic cell death in SK-BR-3 LR cells but not in SK-BR-3 parental cells. Furthermore, palbociclib showed antitumor activity against HER2 targeted therapy resistant patient derived xenograft (PDX) with *CDKN2A* defect and cyclin D1 upregulation.

Conclusion: The changes of cell cycle molecules that were related to G1/S transition was observed in SK-BR-3 LR cells. Deficiency in *CDKN2A* and upregulation of cyclin D1 led to the increased cell cycle progression and proliferation in SK-BR-3 LR cells. CDK4/6 inhibitor palbociclib showed antitumor effect in SK-BR-3 LR cells through modulating cell cycle in vitro and in HER2-directed therapy resistant PDX model. These results suggest that inhibition of cyclin D1 by palbociclib could be an effective strategy for treating lapatinib resistance.

Keywords: Lapatinib, Resistance, CDK4/6 inhibitor, Cell cycle, autophagy

Student number:2017-26288

TABLE OF CONTENTS

ABSTRACT ---------- i

TABLE OF CONTENTS ---------- v

LIST OF TABLES ---------- vi

LIST OF FIGURES ---------- vii

INTRODUCTION ----------1

MATERIALS AND METHODS ----------4

RESULTS ----------19

DISCUSSION ----------62

REFERENCES ----------66

ABSTRACT IN KOREAN ----------70

ACKNOWLEDGEMENT ----------73

LIST OF TABLES

Table 1. mRNA level of SK-BR-3 LR cells versus SK-BR-3 parental cells ----------28

Table 2. Comparison of the degree of methylation in SK-BR-3 parental and LR cells ----------38

LIST OF FIGURES

Figure 1. SK-BR-3 Lapatinib resistance cells were generated by treating lapatinib consistently ----------21

Figure 2. Cell viability after lapatinib treatment in lapatinib resistant SK-BR-3 LR cell ----------22

Figure 3. Proliferation rates of SK-BR-3 parental and LR cells were analyzed ----------23

Figure 4. Cell cycle progression was investigated by FACS---------- ----------24

Figure 5. Alteration of transcriptome expression was observed in SK-BR-3 LR cells ----------27

Figure 6. qPCR data of molecules related in G1/S transition ----------29

Figure 7. Basal expression levels of protein were confirmed by Western blot ----------30

Figure 8. Changes in protein expression after gene knockdown using siRNA----------31

Figure 9. Proliferation rate was analyzed after siRNA transfection ----------32

Figure 10. FACS was conducted to observe alteration of cell cycle progression after siRNA transfection----------33

Figure 11. Genomic DNA copy number was observed by qPCR -----

----------36

Figure 12. *CDKN2A* mRNA level was analyzed by qPCR ---------

----------37

Figure 13. mRNA level was analyzed after 5-aza treatment --------

----------39

Figure 14. Cell viability with palbociclib was analyzed by MTT for 120 hours ----------43

Figure 15. Protein expressions of molecules related in G1/S transition

were inhibited by palbociclib treatment ----------44

Figure 16. Palbociclib inhibited G1/S transition in SK-BR-3 LR cells ----------45

Figure 17. Knockdown of p21 induced cyclin D1 and CDK4 downregulation ----------46

Figure 18. Comparison interaction of cyclin D1 and CDK4/6 between SK-BR-3 parental and LR cells ----------47

Figure 19. Knockdown of p21 altered the level of cyclin D1 complex in the nucleus ----------48

Figure 20. Colony forming assay was conducted to confirm long-term growth inhibition effect of palbociclib ----------51

Figure 21. Modulation of apoptosis, autophagy, senescence signaling ----------52

Figure 22. Sub-G1 population ----------
----------53

Figure 23. Senescence induction was analyzed by β-galactosidase

assay----------54

Figure 24. IFA was conducted to determine whether autophagy was induced by palbociclib ----------55

Figure 25. CCND1 amplification in IMX57 PDX model----------

----------58

Figure 26. IMX57 have similar characteristics with SK-BR-3 LR cells

----------59

Figure 27. Palbociclib treatment was effective in PDX established from HER2 amplified breast cancer patient failed to lapatinib -----60

Figure 28. IHC staining of PDX tumor ----------

----------61

Introduction

HER2 positive breast cancer subtype accounts for 20-25% of breast cancer, and it is highly proliferative by HER2 dependent signal cascade activation. In this signaling cascade, pathways related to proliferation, survival, and invasion such as PI3K/AKT and ERK are present, resulting in tumorigenesis, cellular proliferation, survival, invasion, and metastasis of cancer cells [1, 2]. HER2 directed therapy including trastzumab, pertuzumab, lapatinib and TDM-1 are currently using in the clinic and showed survival benefit for HER2 positive breast cancer [3, 4].

Lapatinib is a dual tyrosine kinase inhibitor which interrupts the HER2/neu and epidermal growth factor receptor (EGFR) pathways in solid tumors. It is used for the treatment of patients with advanced or metastatic breast cancer whose tumors overexpress HER2. Majority of patients who initially respond to the treatment will eventually progress due to acquired resistance. Therefore, it is

necessary to study resistance mechanism and explore strategies to overcome acquired resistance [5-7].

One of the well-known mechanism of lapatinib resistance is cell cycle deregulation. Activation of cyclin D-CDK4/6 complex is one of the mechanisms of lapatinib resistance [8, 9]. During the transition from G1 to S phase Rb played a role as a tumor suppressor at this checkpoint. Rb binds to the transcription factor E2F to inhibit its function. If cyclin D1 forms a complex with CDK4/6, this complex induced inhibitory phosphorylation of Rb. Eventually, it results in E2F-mediated activation, resulting in G1/S transition and promoting cell proliferation [10]. The G1/S cell cycle is destroyed in many cancers, and its dysregulation is known to be a major resistance mechanism [11, 12]. Therefore, CDK4/6 inhibitor that suppresses this pathway is considered to be a novel treatment [9, 13]. Palbociclib has been proposed as a drug targeting G1/S cell cycle progression and is actively used in hormone-receptor positive breast cancer [14, 15]. However, limited information is available for HER2 targeted therapy

resistance HER2 positive breast cancer.

In this study, I investigated that the epigenetic modulation of cyclin-dependent kinase inhibitor (CKI) and the upregulation of cyclin D1 have altered characteristics of SK-BR-3 LR cells and have been shown to be overcome by CDK4/6 inhibitor. And I suggest that CDK4/6 inhibitor, palbociclib can be used as a therapeutic strategy to lapatinib resistant HER2 positive breast cancer.

MATERIALS AND METHODS

1. Reagents and antibodies

Lapatinib and palbociclib were kindly provided by GSK (London, UK) and Pfizer (NY, USA), respectively and they dissolved in dimethyl sulfoxide (DMSO) and stored at -80 ℃. Antibodies against Caspase-3, Cyclin D1, LC3B, pRb, p21 (S780) were purchased from Cell signaling Technology (MA, USA) Antibodies against CDK4, CDK6, E2F-1, p14, Rb, SMP30, Lamin B1 were purchased from Santa Cruz (CA, USA). Antibodies against p16, PARP were purchased from BD Biosciences (CA, USA). Antibodies against thymidylate synthase (TS) were purchased from Abcam (Cambridge, UK). Antibodies against Actin were purchased from Sigma Aldrich (MO, USA).

2. Cell lines and cell cultures

Human HER2 amplified breast cancer cell line (SK-BR-3) was

purchased from the American Culture Collection (Cell Bank; Seoul, South Korea). This cell line was cultured in RPMI 1640 (Thermo Fisher Scientific Inc., MA, USA) supplemented with 10 % fetal bovine serum (Welgene; Gyeongsan-si, South Korea) and 10 μg/mL gentamicin (Cellgro; VA, USA) at 37 ℃ in a 5 % CO_2/95 % air humidified atmosphere.

3. Generations of lapatinib resistant SK-BR-3 cells

SK-BR-3 Lapatinib resistance cell lines were generated by treating lapatinib consistently. Starting from 30 nmol/L and gradually increasing to 10 μmol/L over 7 months. Cell viability assay was conducted to confirm resistance. A clonal selection was conducted and two lapatinib resistant SK-BR-3 clones (LR#2, LR#5) that have similar characteristics with pools of lapatinib resistant were selected. Cells were continuously treated 3 μmol/L of lapatinib in RPMI 1640 medium containing 10 % fetal bovine serum and 10 μg/mL

gentamicin.

4. Cell viability assay

Cells were seeded at a density of 0.2-3 x 10^3 in 100 ㎕/well in 96-well plates and incubated at 37 ℃ in 5 % CO_2/95 % air humidified atmosphere for overnight. Lapatinib and palbociclib treated with gradually increasing concentrations (dose ranges are 0-10 μmol/L and 0-5 μmol/L, respectively). Lapatinib treated for 3 days and palbociclib treated for 5 days and then 50 ㎕ of 3-(4,5-dimethylthiazol-2-yl)-2,5-diphenyltetrazolium bromide solution (Sigma Aldrich) was added and the plates were incubated at 37 ℃ for 4 hours. After removed the media, formazan crystals were dissolved with 150 ㎕ of DMSO. By VersaMax microplate reader (Molecular Devices; CA, USA), the absorbance was measured at 540 nm. The absorbance and IC50 of lapatinib were analyzed with Sigma Plot software (Statistical Package for the Social Sciences, Inc. (SPSs); IL, USA). There were 6

replicates were included in each analysis and independent experiment was repeated at least 3 times.

5. Cell proliferation assay

Cells (1×10^4) were seeded in 6-well plates and incubated overnight at 37 ℃ in 5 % CO_2. The number of cells was counted every 24 hours or 48 hours. The growth rates of each day were normalized with the value of the first day.

6. Cell cycle analysis

Cells were harvested, fixed in 70% ethanol, and then stored at -20 ℃ at least 48 hours. After fixation, they were treated with RNase A (Sigma Aldrich) at 37 ℃ for 1 hour. The cells were stained with 20 μg/mL propidium iodide (Sigma Aldrich) and the contents of DNA were measured by Fluorescence-activated Cell Sorting (FACS)

Calibur flow cytometer (BD Biosciences). 10,000 cells were analyzed in each experimental group.

7. Transcriptome analysis

Total RNA was isolated from sample using Trizol reagent (Molecular research center, Inc., OH, USA) according to the manufacturer's guidelines. Randomly fragmented the purified RNA for sequencing with a short read and reverse-transcribed the cleaved RNA fragment into cDNA. Attached different adapters to both ends of the prepared cDNA fragment and ligated them. cDNA fragments were amplified with PCR. Sequencing service was provided by Macrogen Inc. (Seoul, South Korea). Proceeded with quality control analysis of raw reads obtained through sequencing. Mapped the readers to the reference genome using the HISAT2 (v2.0.5) program considering the splice, and then create the aligned reads, Proceeded with transcript assembly through StringTIe (v1.3.3b) program using information of reference

based on aligned reads. Calculate the amount of expression obtained by transcript quantification of each samples as a normalization value considering transcript length and depth of coverage. Expression profile was extracted by performing within normalization with Fragments Per Kilobase of transcript per Million mapped reads (FPKM) or Read Per Kilobase of Transcript per Million mapped reads (RPKM).

8. Genomic DNA and mRNA extraction, RT-PCR and relative quantitative PCR

Genomic DNA was extracted using the DNeasy purification kit (Qiagen; Hilden, Germany) according to the manufacturer's instructions. RNA was extracted using Trizol reagent (Molecular research center) according to the manufacturer's protocol. 6 μg of total RNA was used for cDNA synthesis with random hexamers. RNA expression level were analyzed by IQTM5 Optical Module (BIO-RAD, CA, USA). Relative qPCR was done with a denaturation

step at 95 ℃ for 10 minutes, followed by 30 cycles of denaturation at 95 ℃ for 1 minute, primer annealing at 60 ℃ for 30 seconds, and primer extension at 72 ℃ for 45 seconds. And a final extension at 72 ℃ for 5 minutes was done and then stored at 4 ℃. The DNA copy number and RNA expression value was normalized with that of Actin. The primer sequence are provided below.

Gene	Primer sequence
CCND1 (gDNA)	5'-TACACCGACAACTCCATCCG-3' 5'-CCATTTGCTGCGAACACA-3'
CDKN2A (p14Arf) (gDNA)	5'-TGATGCTACTGAGGAGCCAGC-3' 5'-AGGGCCTTTCCTACCTGGTC-3'
CDKN2A (p16INK4a) (gDNA)	5'-CTCTGGCAGGTCATGATGATG-3' 5'-CATCTATGCGGGCATGGTTACT-3'
CCND1 (cDNA)	5'-GATGCCAACCTCCTCAACGA-3' 5-GGAAGCGGTCCAGGTAGTTC-3'
CDK4 (cDNA)	5'-CCGACCAGTTGGGCAAAATC-3' 5'-CCATCTCAGGTACCACCGAC-3'
CDK6 (cDNA)	5'-TCACACCGAGTAGTGCATCG-3' 5'-CAAGACTTCGGGTGCTCTGT-3'
CDKN2A (p14Arf) (cDNA)	5'-AGTGAGGGTTTTCGTGGTTCA-3' 5'-TAGACGCTGGCTCCTCAGTA-3'
CDKN2A (p16INK4a) (cDNA)	5'-GACCCCGCCACTCTCACC-3' 5'-CAATCGGGGATGTCTGAGGGA-3'
Actin	5'-GGATGCCACAGGACTCCA-3' 5'-AGAGCTACGAGCTGCCTGAC-3'

9. Western blot analysis

Cells were collected and added extraction buffer (50 mmol/L Tris-Cl (pH 7.4), 150 mmol/L NaCl, 1 % NP40, 0.1 % sodium deoxycholate, 0.1 % sodium dodecyl sulfate (SDS), 50 mmol/L sodium fluoride, 1

mmol/L sodium pyrophosphate, 2 mmol/L phenylmethylsulfonyl fluoride, 1 mg/mL pepstatin A, 0.2 mM leupeptin, 10 μg/mL aprotinin, 1 mmol/L sodium vanadate, 1 mmol/L nitrophenylphosphate, and 5 mmol/L benzamidine) on ice for 30 minutes. Equal amounts of proteins were separated on an 8-15 % SDS-polyacrylamide gel. After the resolved proteins were transferred onto nitrocellulose membranes the blots were probed with primary antibodies at 4 ℃ for overnight. Using enhanced chemiluminescence system according to the manufacturer's protocols (Amersham Biosciences; NJ, USA), antibodies were detected.

10. Methylation sequencing

Genomic DNA was extracted using DNeasy purification kit (Qiagen). DNA fragments were prepared using SureSelect Methyl-Seq Library Prep Kit (Agilent; CA, USA) according to preparation guide. Hybridized genomic DNA using SureSelect Methyl-Seq Kit reagents

(Agilent) and protocol. Hybrids were captured on Dynabeads MyOne streptavidin beads (Thermo Fisher Scientific Inc.; MA, USA), and then eluted. By bisulfate conversion, modified unmethylated C residues and the di-tagged DNA was enriched in PCR, resulting in double-stranded DNA (dsDNA) with the Illumina sequences for use on the HiSeq platform. The sequencing was done by Macrogen Inc. The raw sequence reads are filtered based on quality. The only uniquely mapped reads are selected to sort, index and PCR duplicates are removed with SAMBAMBA (v0.5.9). The methylation ratio of every single cytosine location within on-target region is extracted from the mapping results using 'methylratio.py' script in BSMAP. The results of the coverage profiles were calculated as a number of C / effective CT counts for each cytosine in CpG, CHH and CHG. Each cytosine locus is annotated using table browser function of the UCSC genome browser.

11. Immunoprecipitation

Cells were lysis with pH 7.5 RIPA buffer and pre-clearing with bead. Antibody incubation for overnight at 4 ℃. Adding 50 ㎕ of bead and incubate for 4 hours at 4 ℃. Centrifuge at 2000 rpm and discard the supernatant and washing with 700 ㎕. Repeat washing step 3 times with RIPA buffer and 2 times with DPBS. Add 50 ㎕ of 2X sample buffer and boiling at 100 ℃. Loading samples on gel.

12. Fraction

Resuspend cells with ice-cold lysis buffer with low NaCl concentration. Incubate for 5-10 minutes on ice. Centrifuge at 3000 rpm for 5min and move the supernatant which is cytoplasmic contents to new E-tube. Wash the pellet 3 times with low NaCl buffer and resuspend the pellet with lysis buffer containing high NaCl concentration. Incubate for 30 minutes on ice and centrifuge 13,000

rpm for 10 minutes to obtain supernatant which is nuclear contents.

13. BrdU assay

Cells were treated with 10-20 μmol/L BrdU for 60-90 minutes. Cells were fixed in 70 % ethanol and stored at －20 ℃. After cells were resuspended with phosphate/citric acid buffer, the DNA denaturation was conducted by 4 mol/L HCl for 20 minutes at room temperature. FITC-conjugated anti-BrdU (BD Biosciences) used to investigate the rates of BrdU incorporation. Cells were treated with 7-AAD (BD Biosciences) and fluorescence were analyzed by Fluorescence-activated Cell Sorting (FACS) Calibur flow cytometer (BD Biosciences).

14. siRNA transfection

The siRNA for *CCND1, CDK4, CDK6* was purchased from

Genolution (Seoul, South Korea). p21 siRNA was purchased from Santa Cruz. SK-BR-3 LR cells were transfected with each siRNA at a concentration of 100 or 200 nmol/L using G-fectin (Genolution) according to the manufacturer's instructions. After 24 hours of incubation, cells were re-transfected with siRNA at the same concentration. Cells were harvested after doubling time of SK-BR-3 LR cells. The sequence of *CCND1, CDK4, CDK6* siRNA were 5′-CCACAGAUGUGAAGUUCAUUUCCAAUU-3′, 5′-AAGUAAUCUC UGUAGAAAGAUGGAGGA-3', 5′-UUCUACGAAACAUUUCUGCAA-3'. The sequence of the control siRNA was 5'-AAUUCUCCGAACG UGUCACGUUU-3'.

15. Colony formation assay

Cells were plated at a density of 0.3-3 x 10^3 in 60 mm dishes and incubated at 37 ℃ for overnight. SK-BR-3 parental and LR cells were treated palbociclib every 3 days for 4 weeks or 2 weeks,

respectively. Colonies were fixed with 50 % methanol (Merck; Darmstadt, Germany) and 0.1 % coomassie brilliant blue R-250 solution (Sigma Aldrich) for 2 hours. And the numbers are normalized with the value of control does.

16. β-galactosidase assay

SK-BR-3 Parental and LR cells were treated palbociclib 3 times for 120 hours. Cells were fixed with 1X fixation solution and incubated in β-galactosidase staining solution at 37 ℃ overnight. Procedures were conducted according to the manufacturer's guidelines of β-galactosidase staining kit (Cell signaling Technology). Numbers of senescent cells were counted.

17. Immunofluorescence assay

Cells were seeded on coverslips coated with poly-L-lysine. After 24

hours, cells were treated with palbociclib 3 times for 120 hours. Cells were fixed and permeabilized with 100% methanol for 15 minutes (Merck). Antibody against LC3B (Cell signaling Technology) was added and incubated for overnight. 300 nmol/L of DAPI was stained. Coverslips were mounted onto slides using Faramount aqueous mouting medium (Dako, Glostrup, Denmark) and immunofluorescence was visualized by Zeiss LSM 510 laser scanning microscope.

18. PDX study

PDX experiments were approved from the Institutional Animal Care and Use Committee (IACUC) and conducted in the animal facility of Seoul National University (Seoul, South Korea). Ten NOD scid gamma (NSG) mice were purchased from Central Lab Animal Inc. (Seoul, South Korea) to confirm that palbociclib works effectively to HER2 targeted therapy resistant breast cancer that have high cyclin D1 and low *CDKN2A* in the PDX model. Patient tissues were

transplanted subcutaneously into each mouse. When the tumor volume reached 150 mm^3, the mice were divided into 2 groups randomly. One group received vehicle (pH 4.0 sodium acetate 50 mmol/L) and the other group were treated palbociclib (150 mg/kg) via oral gavage once daily for 28 consecutive days. Tumor volume was calculated using the formula : (wide^2 x height)/2. After 28 days, the mice were sacrificed with CO_2 and the tumor tissues were excised for further analysis.

19. Statistical analysis

Data were analyzed using SigmaPlot version 10.0 (SPSs). Results were expressed as the mean ± standard deviation (S.D.) or standard error (S.E.). A two side Student's t-test was used when appropriate. p-values less than 0.05 were considered statistically significant and those less than 0.1 were considered meaningful. All experiments were conducted in duplicate or triplicated and repeated at least twice.

Results

1. The accelerated cell proliferation and cell cycle progression were exhibited in lapatinib resistance cells

Lapatinib resistant cell line was established from human HER2 amplified SK-BR-3 breast cancer cell line. Although SK-BR-3 cell line was originally highly sensitive to lapatinib, by consistently treating lapatinib, SK-BR-3 lapatinib resistance (LR) cell line acquired resistance to lapatinib. Two lapatinib resistant clones (LR clone #2, #5) were selected by clonal selection (Fig. 1) and confirmed that their characteristics were similar to their pool. Resistance to lapatinib of SK-BR-3 LR cells was confirmed by growth inhibitory assay (Fig. 2). SK-BR-3 LR cells and its clones had different characteristics compared to SK-BR-3 parental cells, especially in terms of proliferation rates and cell cycle progression (Fig. 3, 4). They showed that accelerated proliferation and cell cycle progression.

These results indicate that SK-BR-3 LR cells are resistant to

lapatinib and had a new trait in comparison with the SK-BR-3 parental cell line. And also, I anticipated that I could find a mechanism to overcome the lapatinib resistance by analyzing these changed properties in SK-BR-3 LR cells.

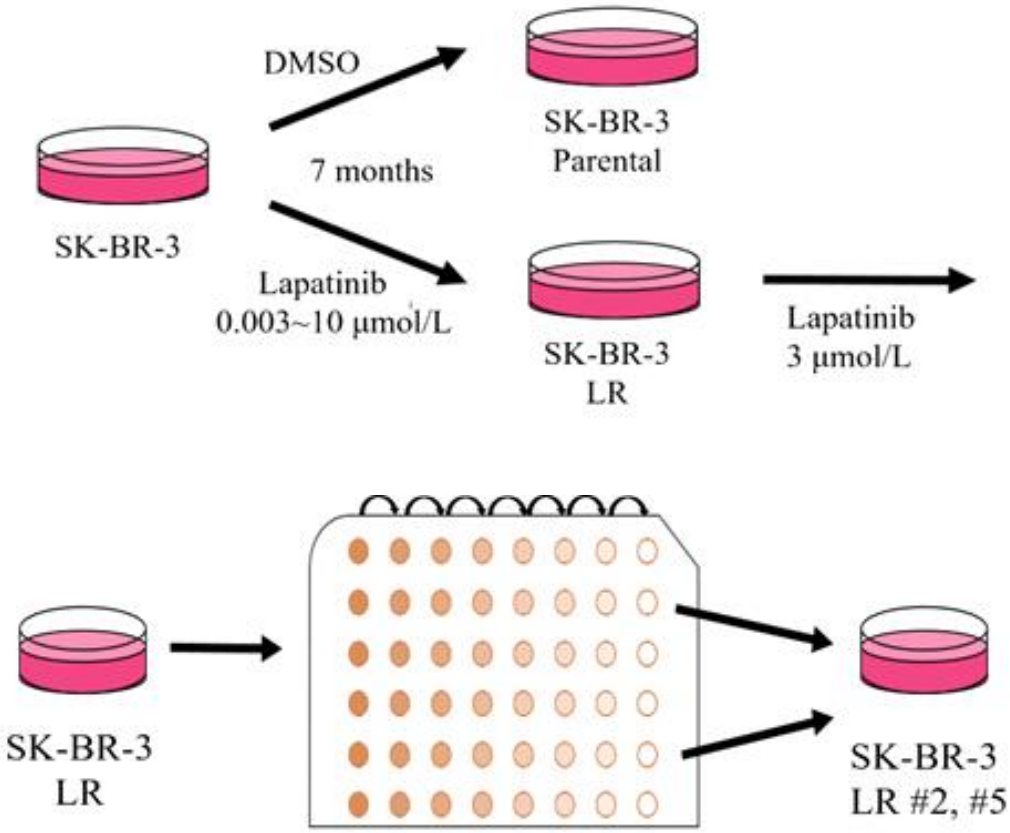

Fig 1. SK-BR-3 Lapatinib resistance cells were generated by treating lapatinib consistently.

Lapatinib resistance cells were established by treating lapatinib for 7 months. Parental cells were generated by DMSO treatment for the same period. A clonal selection was conducted.

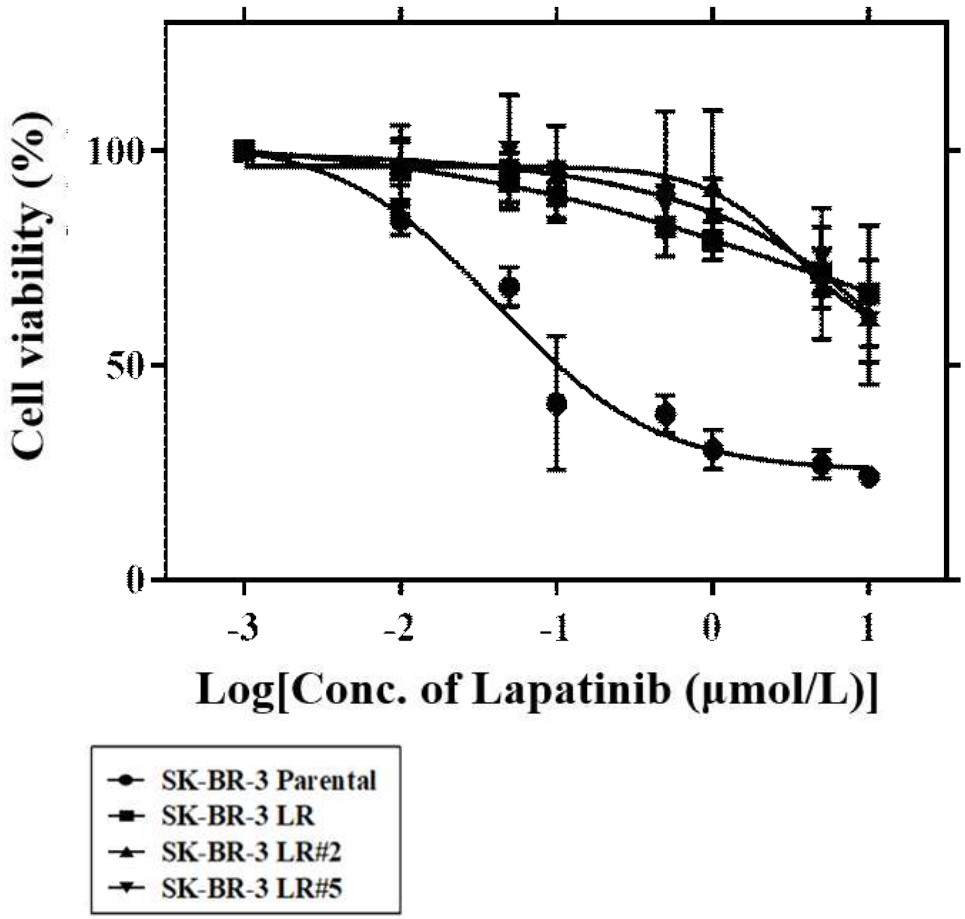

Figure 2. Cell viability after lapatinib treatment in lapatinib resistant SK-BR-3 LR cells.

Growth inhibition was analyzed by the MTT assay. Lapatinib was treated for 72 hours as indicated lapatinib concentrations.

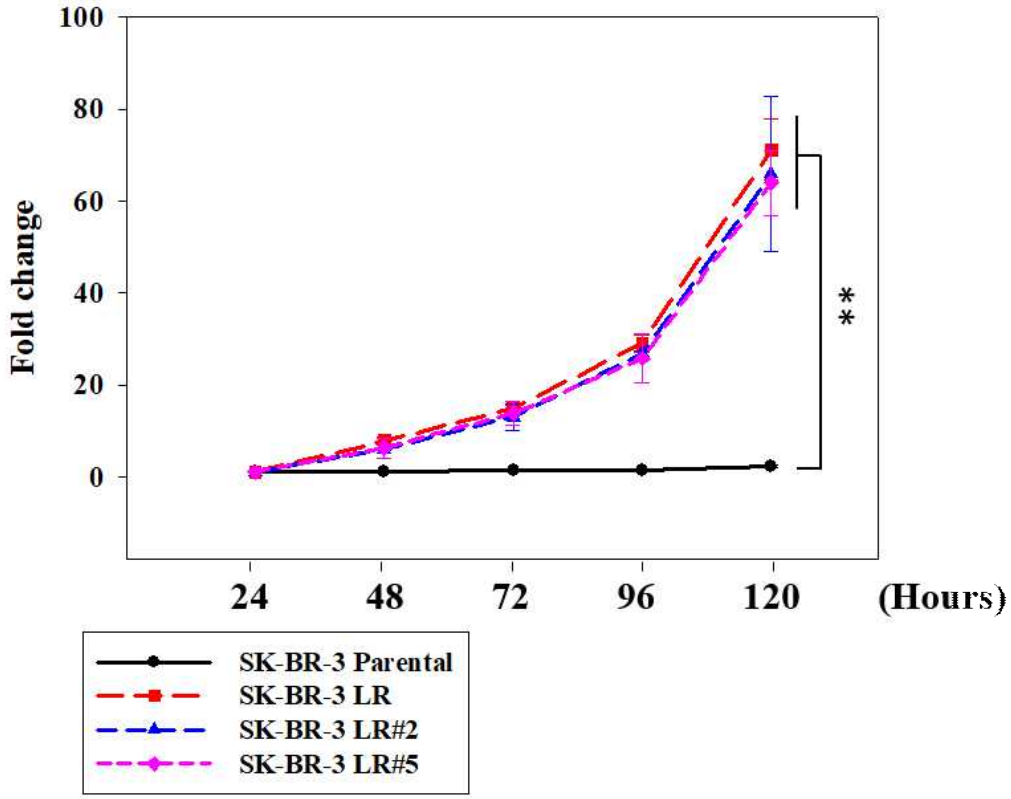

Figure 3. Proliferation rates of SK-BR-3 parental and LR cells were analyzed.

Proliferation rates were measured every 24 hours for 5 days. Cell number was normalized with that of 24 hours. (** $p<0.05$).

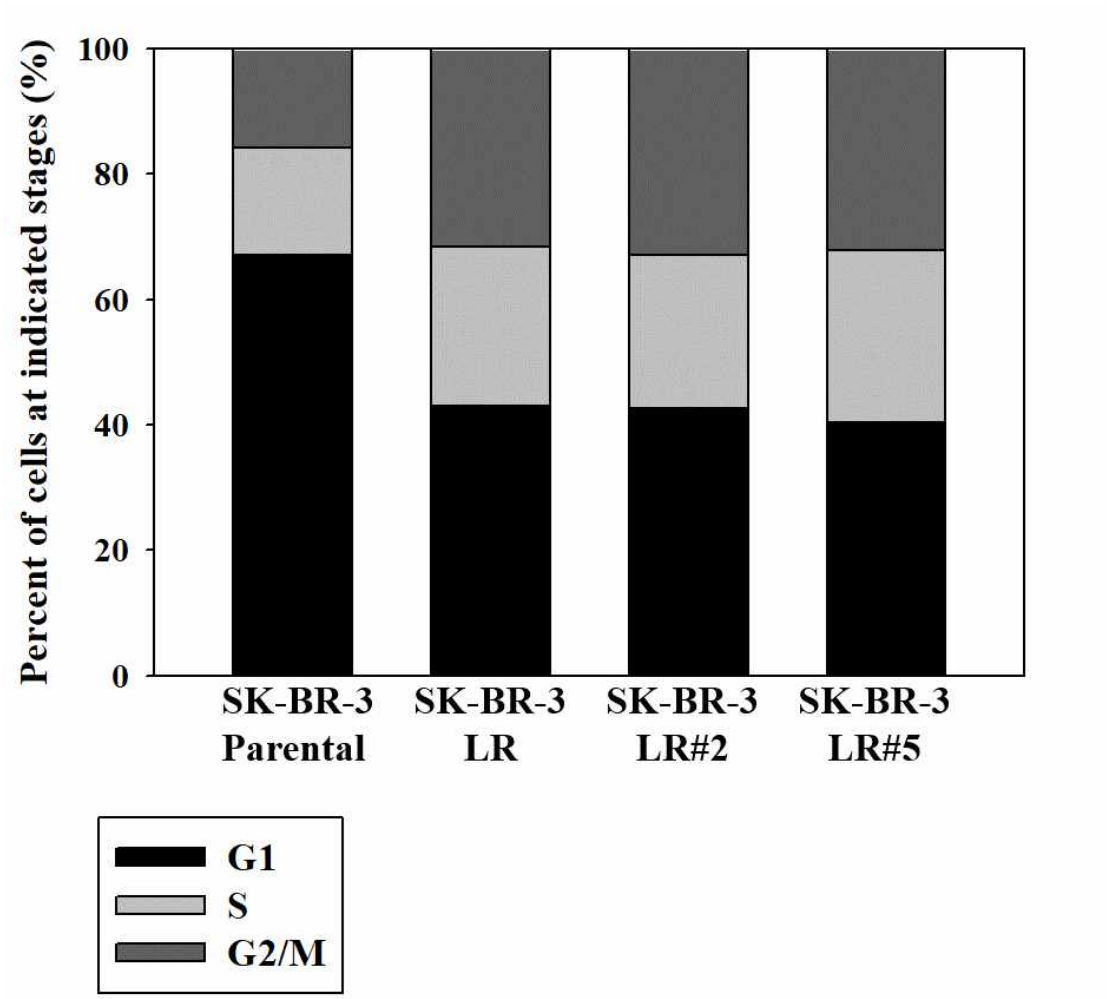

Figure 4. Cell cycle progression was investigated by FACS.

Cells were harvested after cell cycle arrest for 6 hours and released for additional 24 hours. Identified changes in cell cycle progression during the same time period.

2. Expression of cell cycle-related molecules altered in SK-BR-3 LR cells.

Since cell cycle progression and cell proliferation rates were increased in SK-BR-3 LR cells compared to parental cells, it was expected that there would be changes related to the cell cycle. Transcriptome data showed that the altered expression of the molecules related to the G1/S transition was observed (Fig. 5, Table 1). *CCND1* and *CDK6* mRNA levels were upregulated not only in SK-BR-3 LR cells but also in LR clones by qPCR (Fig. 6). Protein expression was observed to follow mRNA expression pattern (Fig. 7).

To determine which molecules among cyclin D1, CDK4, and CDK6 had the greatest effect on the altered characteristics of SK-BR-3 LR cells. To confirm this, siRNA transfection was used to observe whether changes in proliferation rate or cell cycle progression induced when each molecule was knocked down.

As a result, pRb and E2F-1 protein expression were decreased by

knockdown of *CCND1, CDK4*, and *CDK6* (Fig. 8). However, the proliferation rate and cell cycle progression were reduced only when *CCND1* was suppressed (Fig. 9, 10). These data suggest that cyclin D1 is a factor that causes changes in the characteristics of SK-BR-3 LR cells.

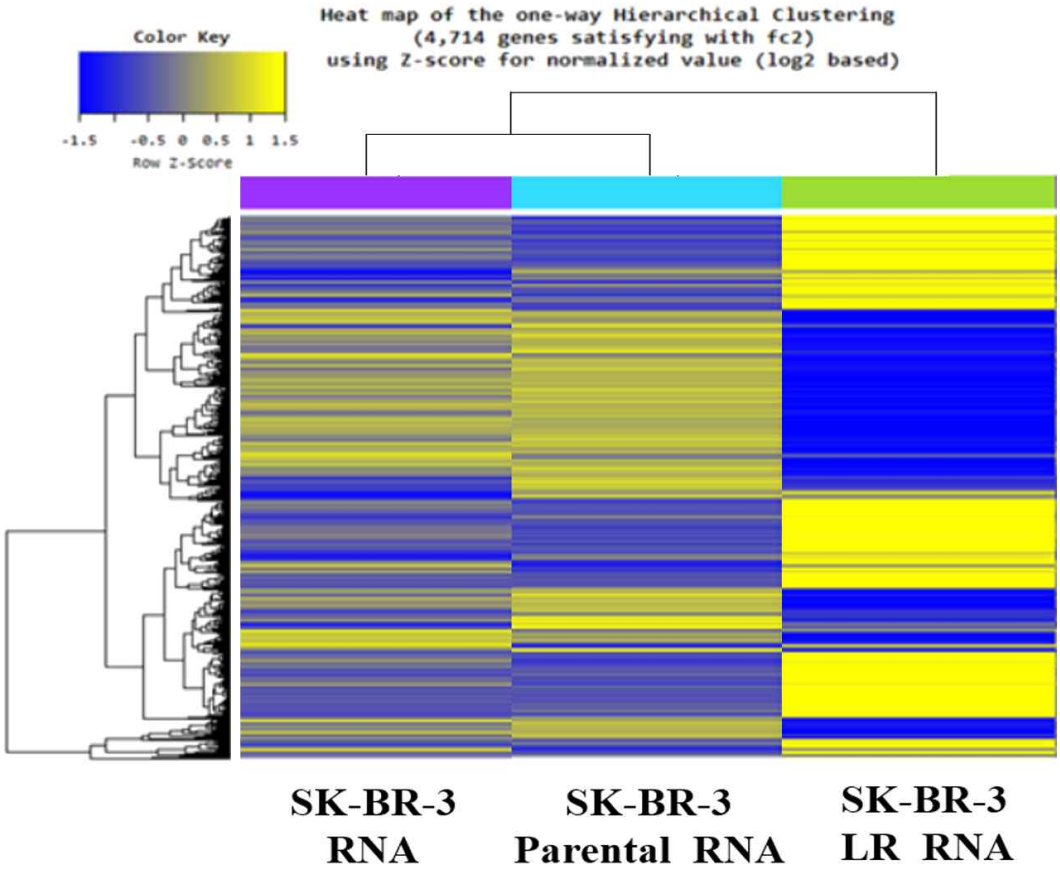

Figure 5. Alteration of transcriptome expression was observed in SK-BR-3 LR cells.

The difference between SK-BR-3 parental and LR cells were analyzed by RNA sequencing. Among the three cell lines (SK-BR-3, SK-BR-3 Parental, SK-BR-3 LR), it was confirmed that remarkable changes induced in SK-BR-3 LR cells.

Table 1. mRNA level of SK-BR-3 LR cells versus SK-BR-3 parental cells.

Transcript ID	Gene symbol	Description	LR-RNA/PR-RNA (fold change)
NM_053056	*CCND1*	cyclin D1	2.517709
NM_001136017, NM_001136125, NM_001136126, NM_001287427, NM_001287434, NM_001760	*CCND3*	cyclin D3	2.094686
NM_057749	*CCNE2*	cyclin E2	2.179299
NM_000075	*CDK4*	cyclin dependent kinase 4	2.168217
NM_001145306, NM_001259	*CDK6*	cyclin dependent kinase 6	4.554441
NM_000389, NM_001220777, NM_001220778, NM_001291549, NM_078467	*CDKN1A*	cyclin dependent kinase inhibitor 1A	5.729495
NM_004064	*CDKN1B*	cyclin dependent kinase inhibitor 1B	3.374305
NM_000077, NM_001195132, NM_058195, NM_058197	*CDKN2A*	cyclin dependent kinase inhibitor 2A	-9.643001
NM_001262, NM_078626	*CDKN2C*	cyclin dependent kinase inhibitor 2C	-5.488531
NM_001950	*E2F4*	E2F transcription factor 4	3.013315
NM_001083588, NM_001083589, NM_001951	*E2F5*	E2F transcription factor 5	5.230464
NM_00321	*RB1*	RB transcriptional corepressor 1	3.352513

The molecules related to G1/S transition were changed.

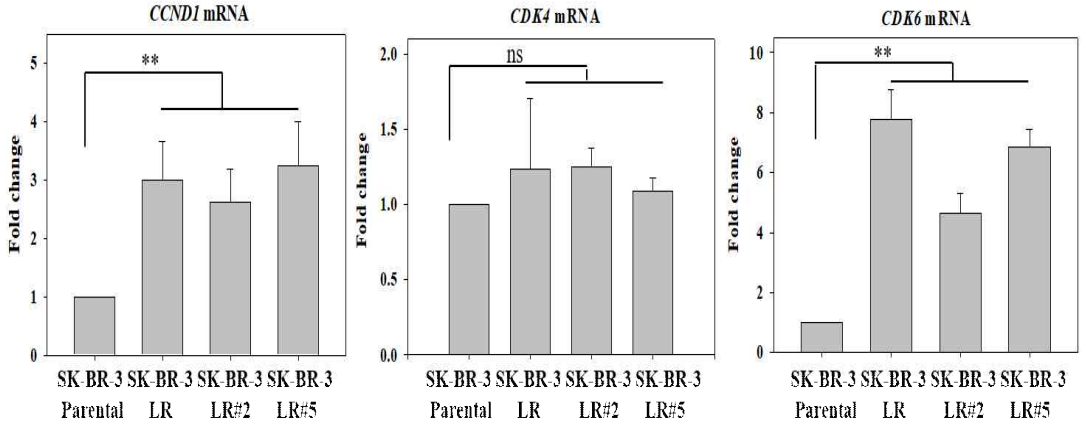

Figure 6. qPCR data of molecules related in G1/S transition.

CCND1 and *CDK6* were upregulated in SK-BR-3 LR cells. mRNA expression was renormalized by the value of SK-BR-3 parental cells. (**$p<0.05$).

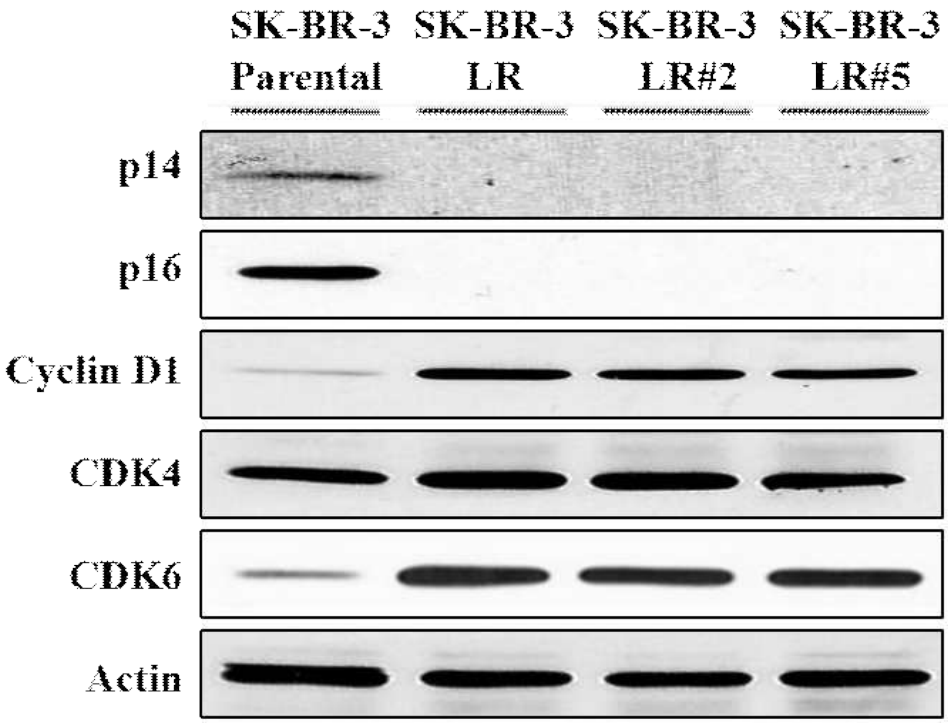

Figure 7. Basal expression levels of protein were confirmed by Western blot.

In SK-BR-3 LR cells, protein level of cyclin D1, CDK6 were increased and p14, p16 levels were suppressed as seen at the mRNA level. Actin was used as loading control.

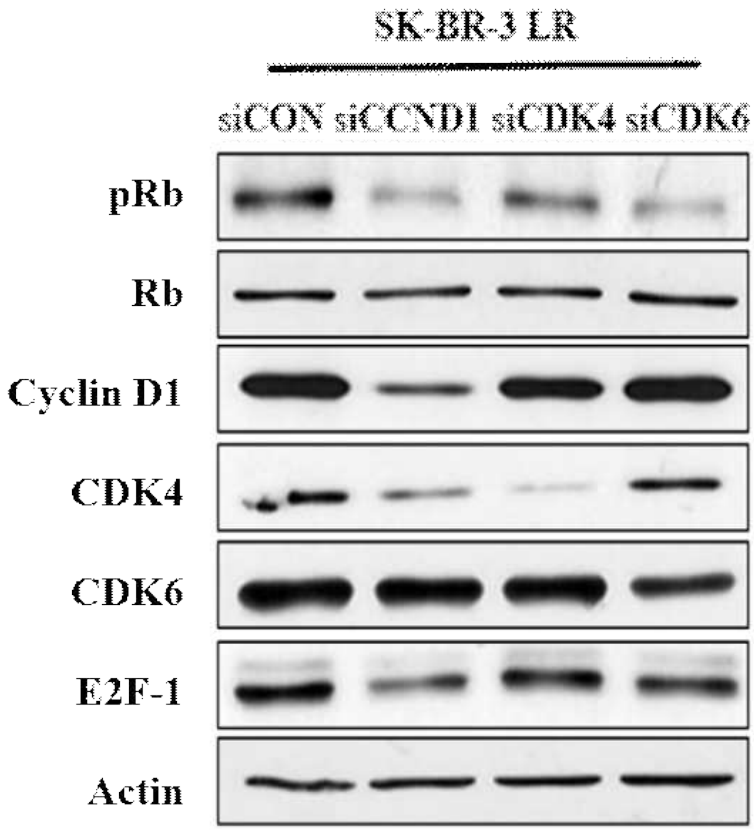

Figure 8. Changes in protein expression after gene knockdown using siRNA.

Cyclin D1, CDK4, CDK6 knockdown induced downregulation of pRb and E2F-1. pRb downregulation was most prominent after cyclin D1 knockdown using si*CCND1* transfection.

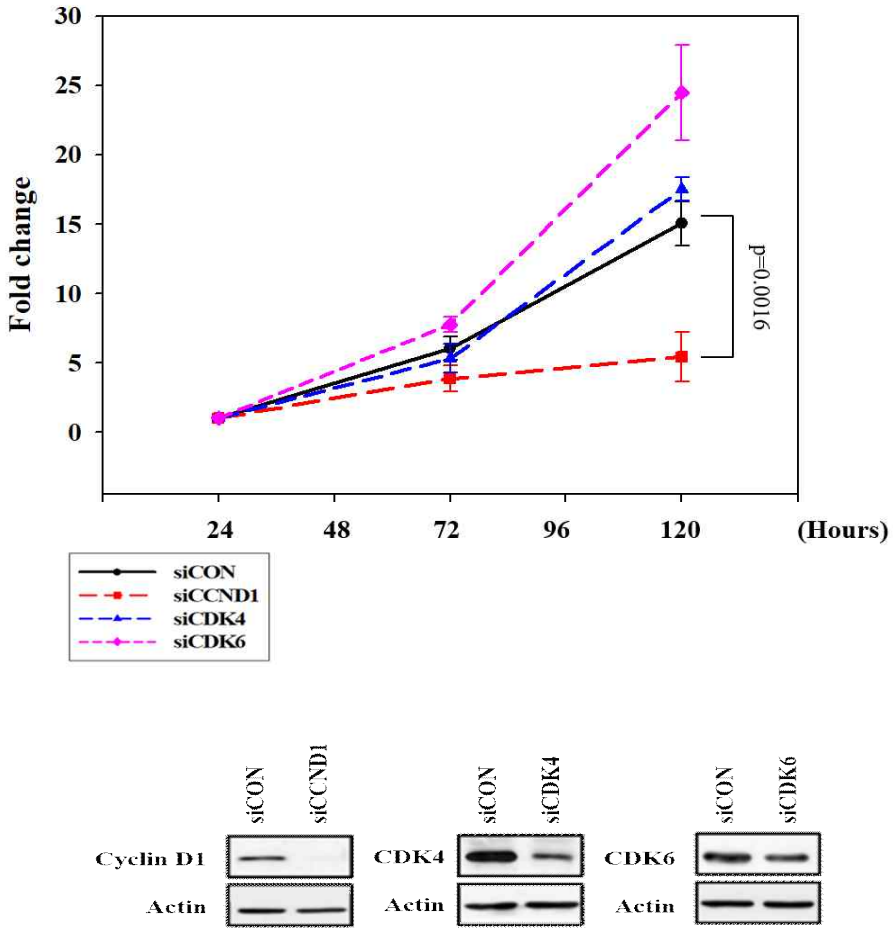

Figure 9. Proliferation rate was analyzed after siRNA transfection.

Proliferation rate was reduced only after si*CCND1* transfection in SK-BR-3 LR cells. The number of cells was counted once every two days and renormalized with the number of 24 hours. The cells were harvested at 120 hours timepoint of proliferation assay to confirm knockdown.

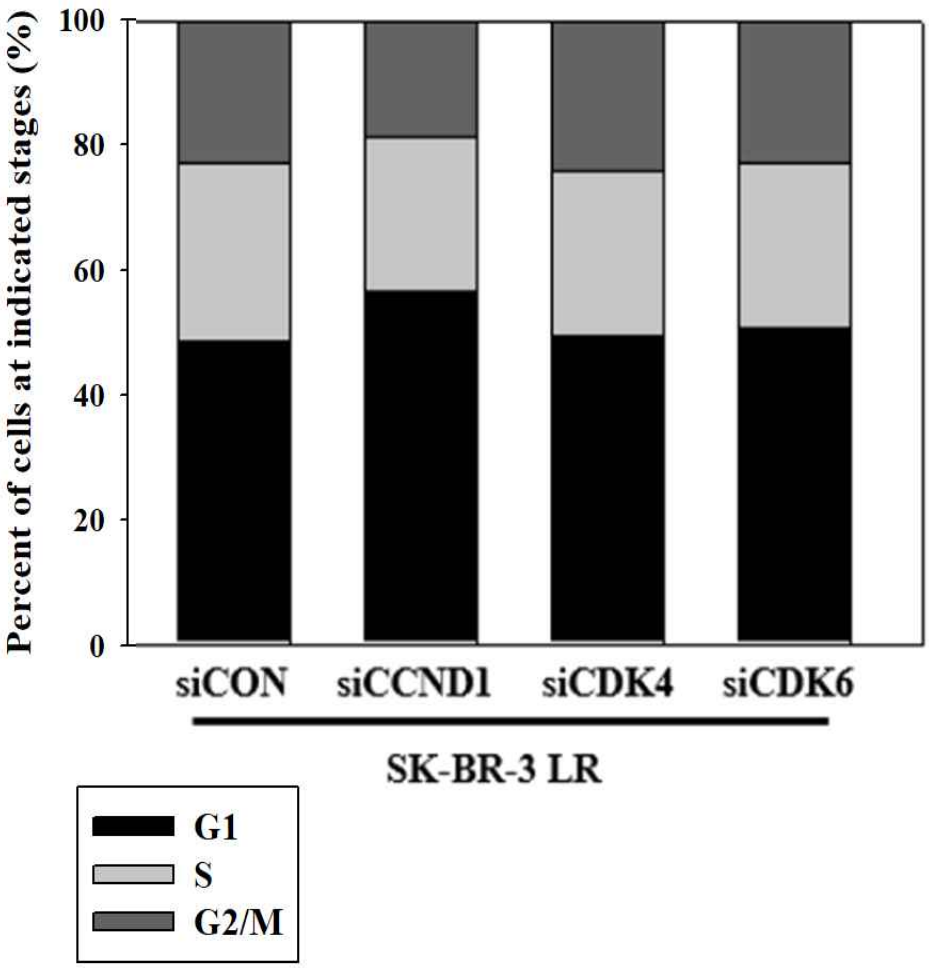

Figure 10. FACS was conducted to observe alteration of cell cycle progression after siRNA transfection.

After si*CCND1* transfection, fraction of cells in G1 phase was increased whereas fraction of S and G2/M phase was decreased.

3. Upregulation of cyclin D1 induced due to defect of *CDKN2A*

I tried to identify the cause of cyclin D1 upregulation. First, I checked the copy number of genomic DNA and confirmed that there was no evidence of genomic DNA amplification (Fig 11). Interestingly, *CDKN2A*, inhibitor of cyclin D-CDK4/6 complexes, was defected at the mRNA level (Fig 12). *CDKN2A* suppression was also observed at the protein level (Fig 7). These changes were also not associated with the genomic DNA copy number (Fig 11) and methylation sequencing revealed that histone methylation increased at SK-BR-3 LR cells compared to the parental cells (Table 2). These were confirmed by 5-aza treatment, methyltransferase inhibitor. 5-aza treatment resulted in an increase of *CDKN2A* mRNA levels in SK-BR-3 LR cells (Fig 13).

Through these data, I could confirm that changes in G1/S cell cycle molecules, such as *CCND1* upregulation and epigenetic

suppression of *CDKN2A* are the mechanisms of accelerated proliferation and cell cycle progression in SK-BR-3 LR cells.

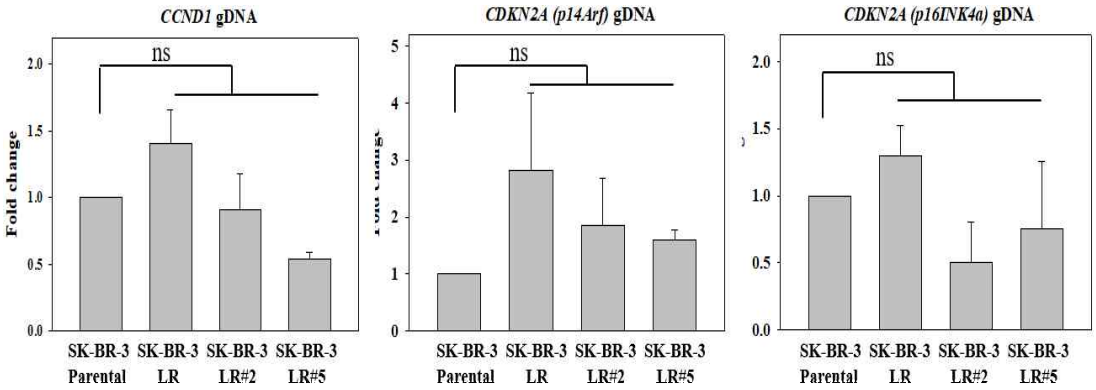

Figure 11. Genomic DNA copy number was observed by qPCR.

CCND1, CDKN2A copy number alteration were not observed in SK-BR-3 LR cells compared to parental cells.

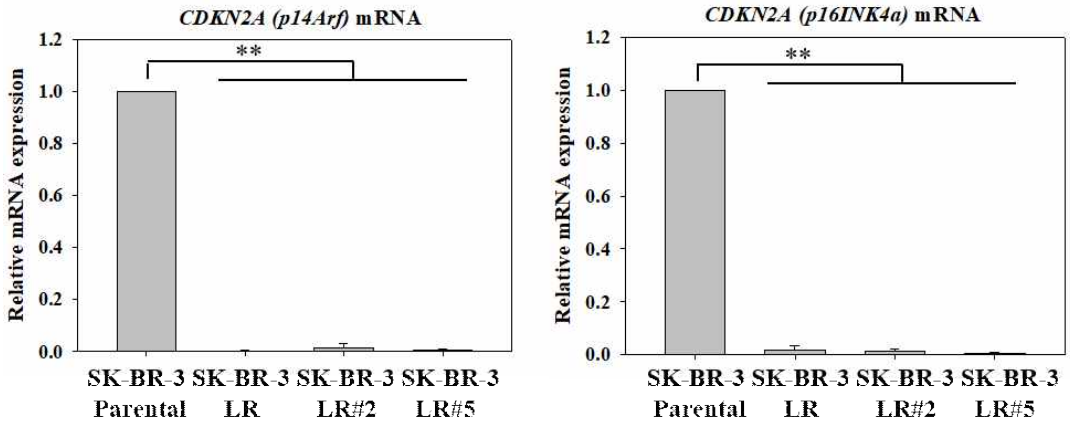

Figure 12. *CDKN2A* mRNA level was analyzed by qPCR.

CDKN2A was defected in SK-BR-3 LR cells. mRNA expression was renormalized by the value of SK-BR-3 parental cells. (**$p<0.05$).

Table 2. Comparison of the degree of methylation in SK-BR-3 parental and LR cells.

Gene symbol	SK-BR-3 Parental cells	SK-BR-3 LR cells
CDK6	0.13579	0.19642
CCND1	0.34739	0.42205
CDKN2A	0.54884	0.95826

CDKN2A was fully methylated in SK-BR-3 LR cells. A value of 1 means fully methylated in CpG sites of overall gene. The closer the value is to 1, the more methylation occurs.

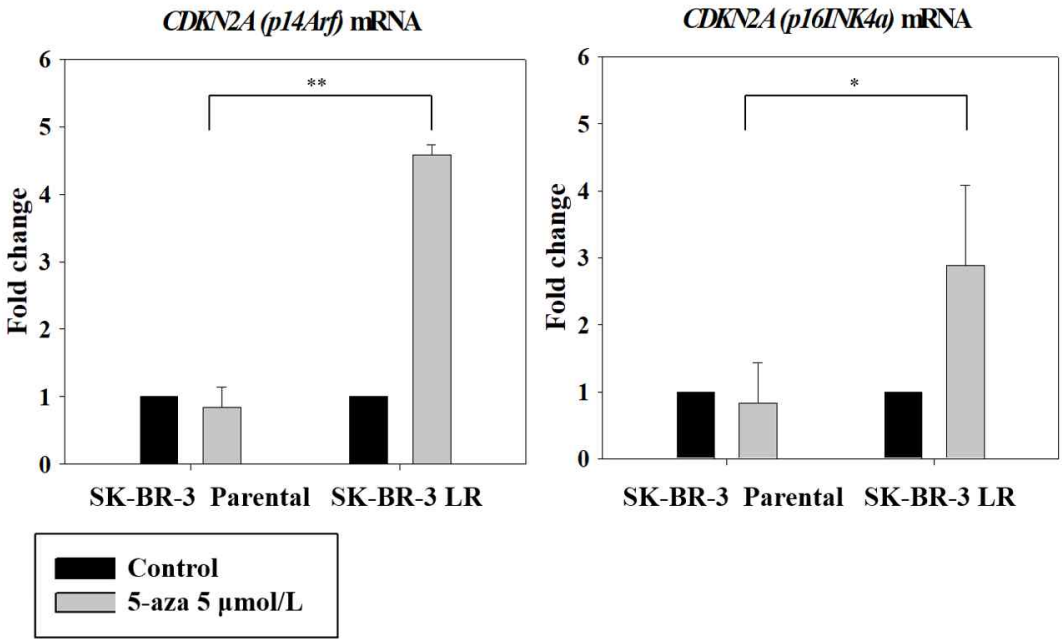

Figure 13. mRNA level was analyzed after 5-aza treatment.

After 5-aza treatment, the mRNA level of *CDKN2A* genes were increased in SK-BR-3 LR cells. Expression of mRNA level after 5 μmol/L of 5-aza treatment was normalized with control (0 μmol/L) by fold change. (**$p<0.05$, *$p<0.1$).

4. Palbociclib induced G1 cell cycle arrest in SK-BR-3 LR cells.

I hypothyzed that CDK4/6 inhibitor which inhibits cyclin D activity might be effective in suppressing the growth of SK-BR-3 LR cells. Palbociclib, a CDK4/6 inhibitor, was observed to be more effective in SK-BR-3 LR cells than SK-BR-3 parental cells (Fig. 14).

Next, I investigated the mechanisms of palbociclib effects. Considering that the effect of palbociclib decreases as the cell doubling time passes, I treated palbociclib during each cell's doubling time. As a result, it was confirmed that G1 arrest was induced by palbociclib through decrease of pRb and E2F-1. I observed that the degree of DNA synthesis was reduced, and it was confirmed by the reduction of thymidylate synthase (TS) expression (Fig. 15). When I observed the degree of S phase incorporation by BrdU assay under the same conditions, I found that cell cycle progression was

significantly reduced by palbociclib in SK-BR-3 LR cells (Fig 16).

In addition, I investigated the cause of the cyclin D1 upregulation despite of palbociclib treatment. Previous studies have shown that p21, a CDK inhibitor, may induce accumulation of cyclin D1 [16-18]. GSK3β induces nuclear export of cyclin D1 which is phosphorylated at the threonine 286 site. However, when p21 binds to cyclin D1, it overrides this site and stabilizes the cyclin D1-CDK4/6 complex in the nucleus [19-21]. p21 was increased after palbociclib treatment in SK-BR-3 LR cells (Fig 15). When p21 was knocked down, cyclin D1 and CDK4 expression were decreased. Conversely, when p21 upregulated by palbociclib treatment, cyclin D1 and CDK4 expression were also induced (Fig 17). The interaction between cyclin D1 and p21 was increased in SK-BR-3 LR cells compared with parental cells, and the interactions between cyclin D1 and CDK4, CDK6 were also increased. However, p21 suppression in SK-BR-3 LR cells reduced the interaction of cyclin D1-CDK6 complexes, indicating that cyclin D1 upregulation induced by palbociclib was due to p21 (Fig 18).

Knockdown of p21 also resulted in a decrease of cyclin D1, CDK4, CDK6 in the nucleus (Fig 19).

These findings indicate that palbociclib inhibited cellular proliferation by inducing G1 cell cycle arrest.

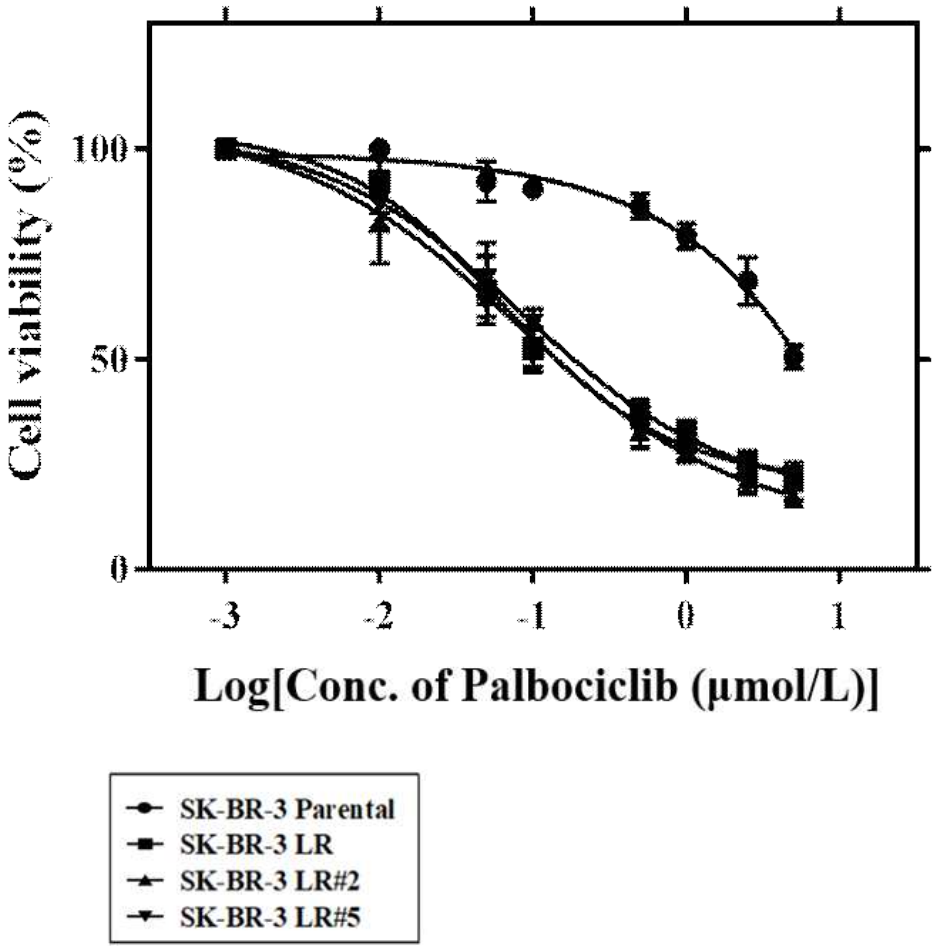

Figure 14. Cell viability with palbociclib was analyzed by MTT for 120 hours.

After 120 hours treatment of palbociclib, cell viability of SK-BR-3 LR cells were remarkably decreased compared to SK-BR-3 parental cells.

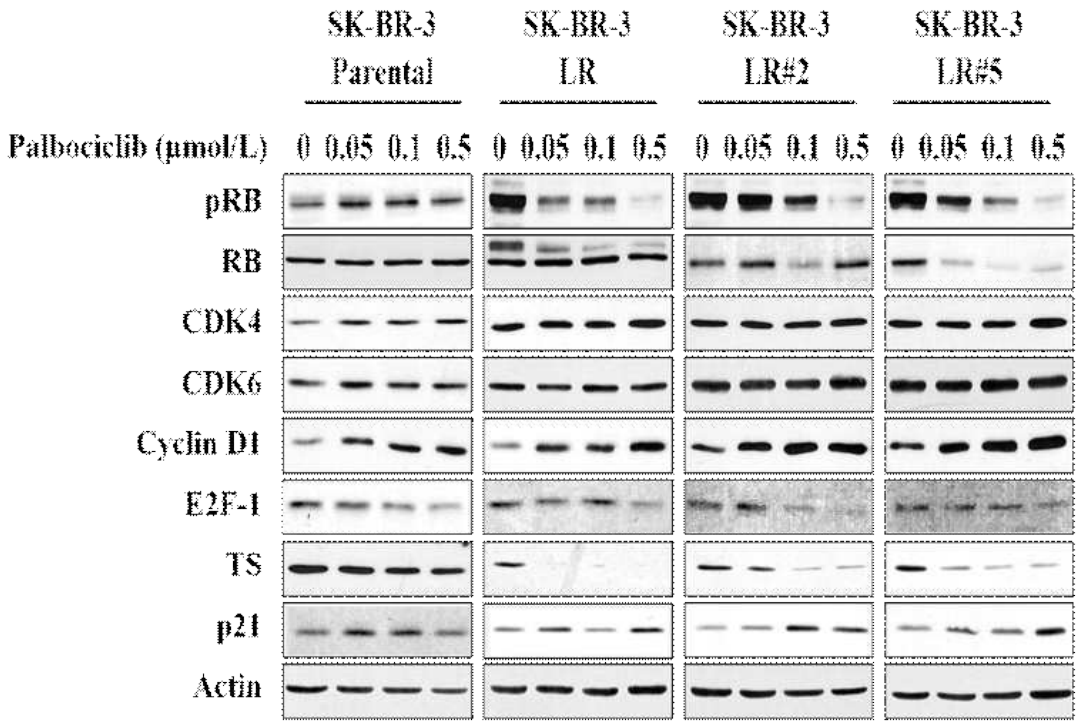

Figure 15. Protein expressions of molecules related in G1/S transition were inhibited by palbociclib treatment.

pRb and E2F-1 protein expression were downregulated after palbociclib treatment. Thymidylate synthase expression was also decreased by palbociclib treatment. Duration of palbociclib treatment was matched with doubling time of each cell's (Parental : 51 hours, LR : 14 hours).

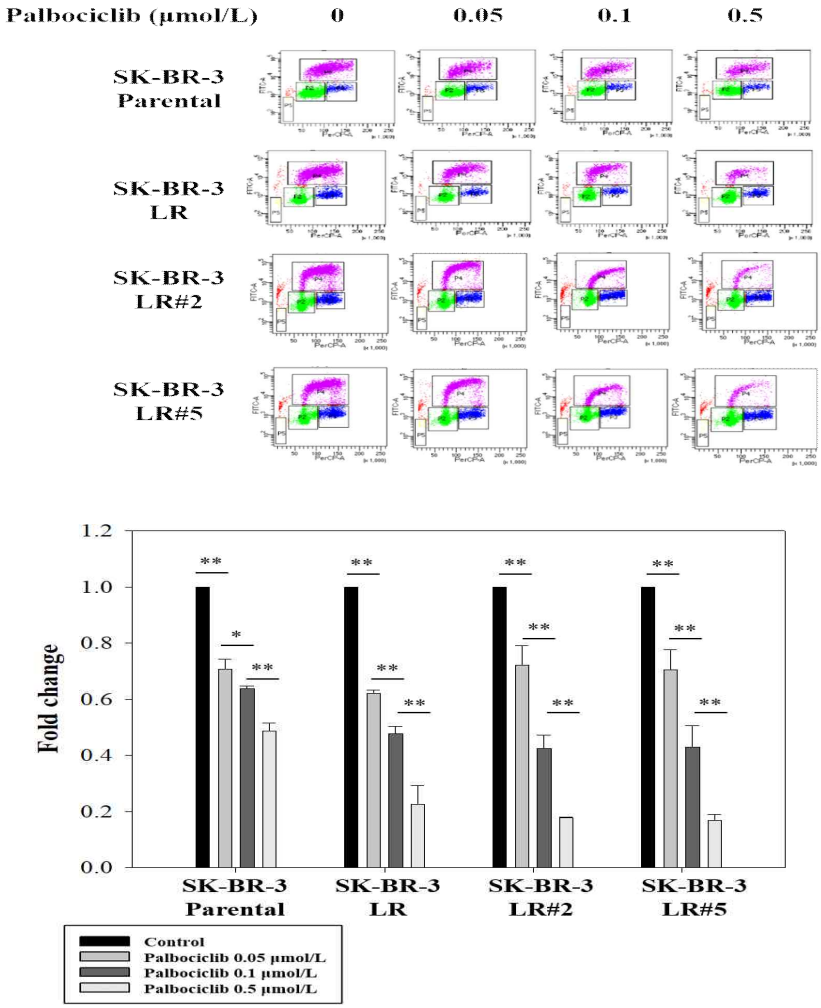

Figure 16. Palbociclib inhibited G1/S transition in SK-BR-3 LR cells.

In SK-BR-3 LR cells, palbociclib induced G1 arrest and reduced S phase incorporation. Palbociclib treated for each cell's doubling time. (**p<0.05, *p<0.1)

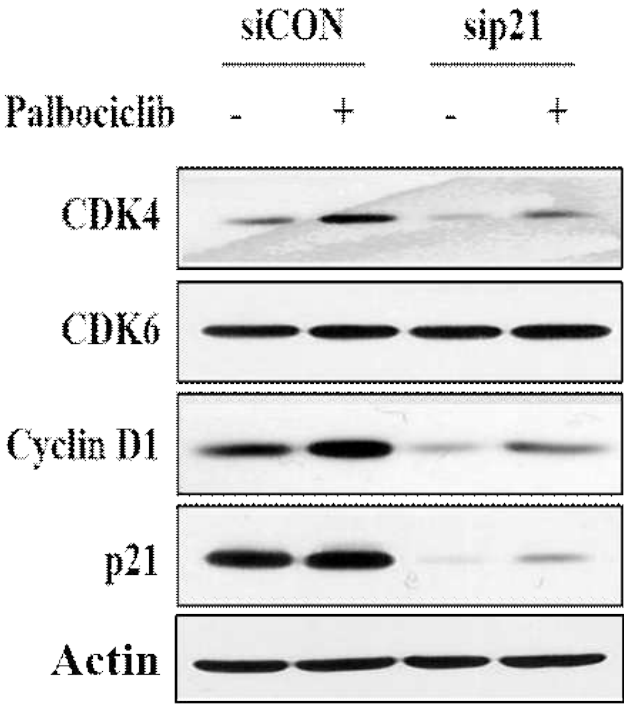

Figure 17. Knockdown of p21 induced cyclin D1 and CDK4 downregulation.

When p21 was downregulated by siRNA, cyclin D1 and CDK4 also suppressed. When palbociclib was treated, p21 was slightly increased, and cyclin D1 and CDK4 followed the tendency.

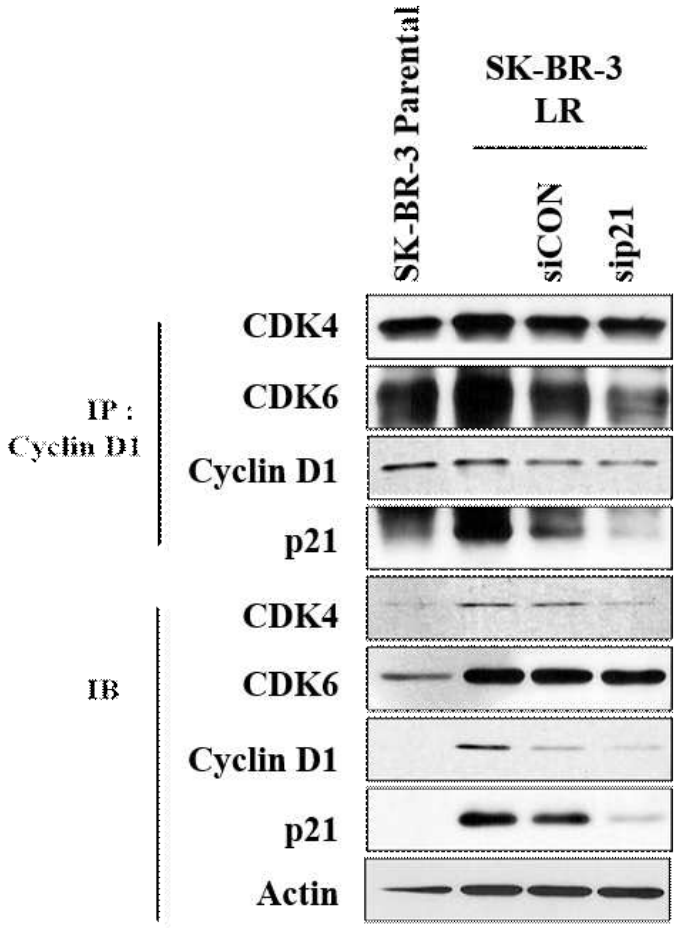

Figure 18. Comparison interaction of cyclin D1 and CDK4/6 between SK-BR-3 parental and LR cells.

In SK-BR-3 LR cells, the interaction between cyclin D1-CDK6 or p21 was increased compared to parental cells. Cyclin D1-CDK6 interaction decreased after p21 suppression by siRNA.

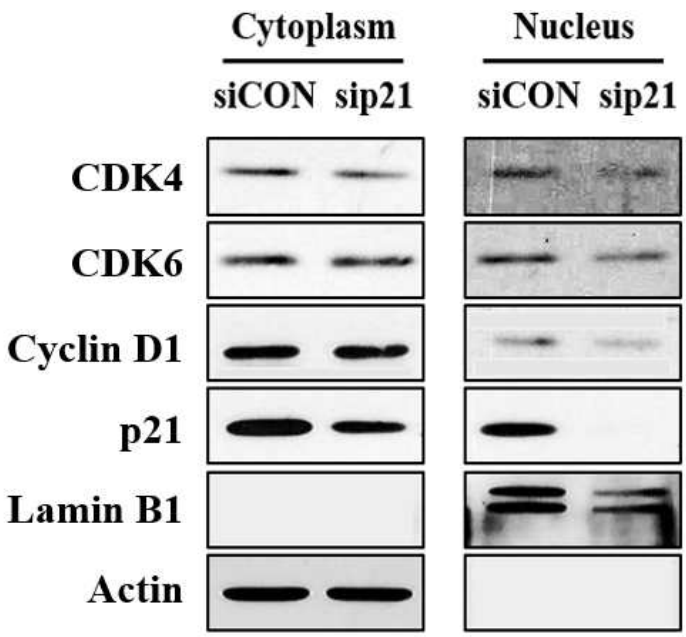

Figure 19. Knockdown of p21 altered the level of cyclin D1 complex in the nucleus.

Knockdown of p21 by siRNA induced downregulation of CDK4, CDK6, and cyclin D1 in the nucleus.

5. Autophagy was induced by palbociclib in SK-BR-3 LR cells.

The colony formation assay was performed to determine whether palbociclib showed anti-proliferative effect in long-term culture system. As a result, I observed that the colony formation was significantly reduced by palbociclib treatment in the SK-BR-3 LR cells, and thus palbociclib was confirmed to be effective also in the long-term (Fig. 20).

I assumed the antitumor effect of palbociclib observed in SK-BR-3 LR cells is mediated by apoptotic cell death [22, 23]. However, despite the cell death was induced by palbociclib in SK-BR-3 LR cells, neither the sub-G1 population nor the cleaved forms of PARP and caspase-3 were observed (Fig 21, 22).

Palbociclib has been known to exert its effects through senescence through several previous studies [24-26]. I investigated whether

palbociclib causes senescence in SK-BR-3 LR cells. I could not observe any increase in SMP30 (Fig. 21) [27], a senescence marker, and confirmed that no stained cells were observed even though β-galactosidase assay (Fig. 23), another senescence confirmation method, was performed. These data provide evidence that the effect of palbociclib does not occur through senescence and apoptosis in SK-BR-3 LR cells.

To determine which of cell death mechanisms the effect of palbociclib is occupied by, I tested whether autophagy can be induced by palbociclib in SK-BR-3 LR cells [23, 25]. Treatment of palbociclib in SK-BR-3 LR cells showed an increase in autophagy marker, LC3-II (Fig. 21) and LC3 puncta formation (Fig. 24).

Taken together, I conclude that palbociclib exerts its effects through autophagy in SK-BR-3 LR cells.

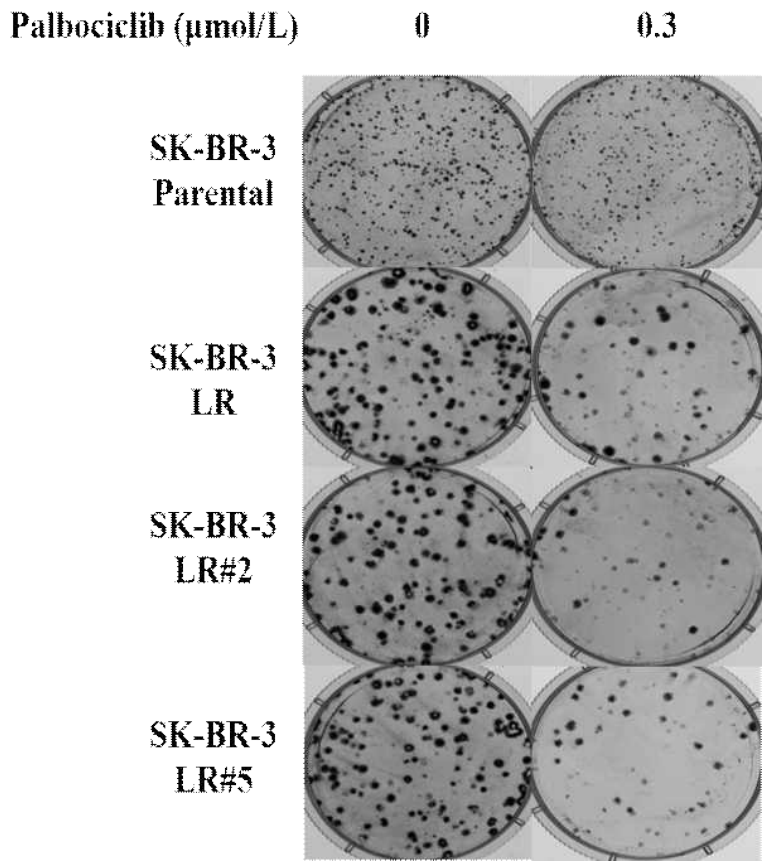

Figure 20. Colony forming assay was conducted to confirm long-term growth inhibition effect of palbociclib.

SK-BR-3 parental and LR cells were subjected to colony formation assay with three times of palbociclib treatment considering each cell's doubling time. In SK-BR-3 LR cells, colony formation rates were remarkably reduced by palbociclib.

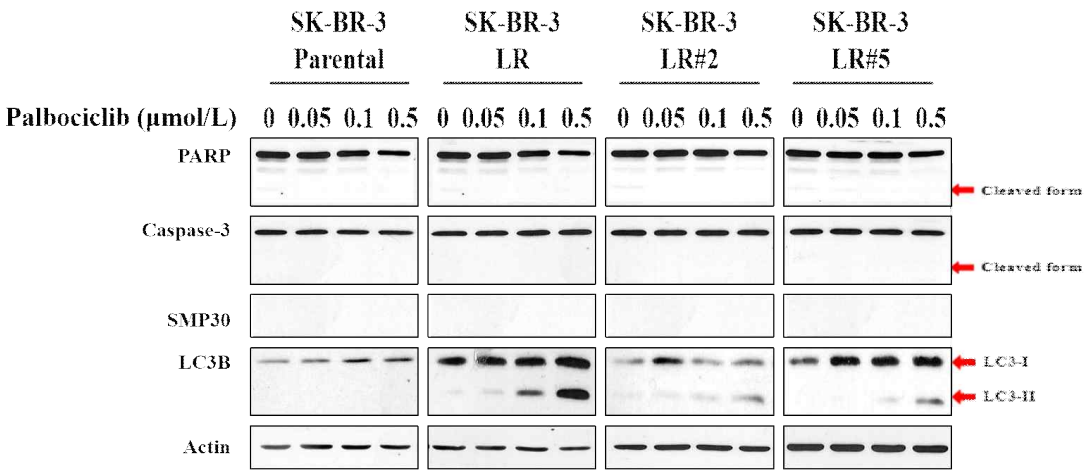

Figure 21. Modulation of apoptosis, autophagy, senescence signaling.

There was no increase in cleaved PARP, cleaved caspase-3 and SMP30 by palbociclib. LC3-II expression was induced by palbociclib in dose-dependent manner. Palbociclib was treated 3 times for 120 hours.

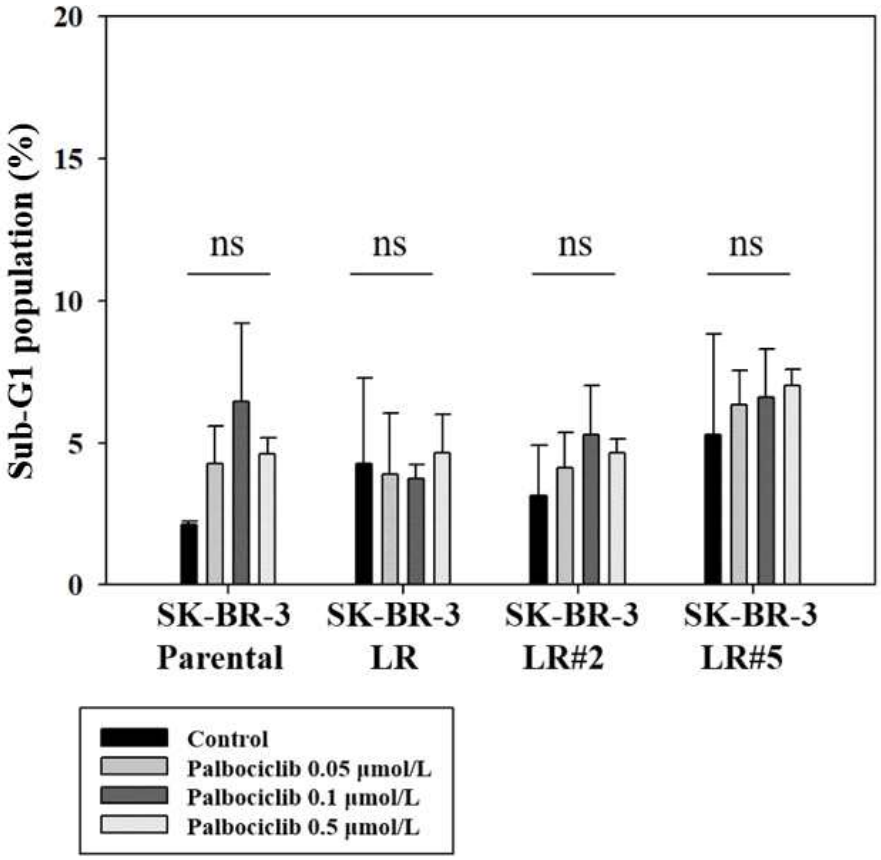

Figure 22. Sub-G1 population.

Palbociclib was added for every 48 hours for 120 hours. Sub-G1 population was not statistically significantly increased in SK-BR-3 LR cells by palbociclib treatment compared to parental cells. (*ns : no statistical significance)

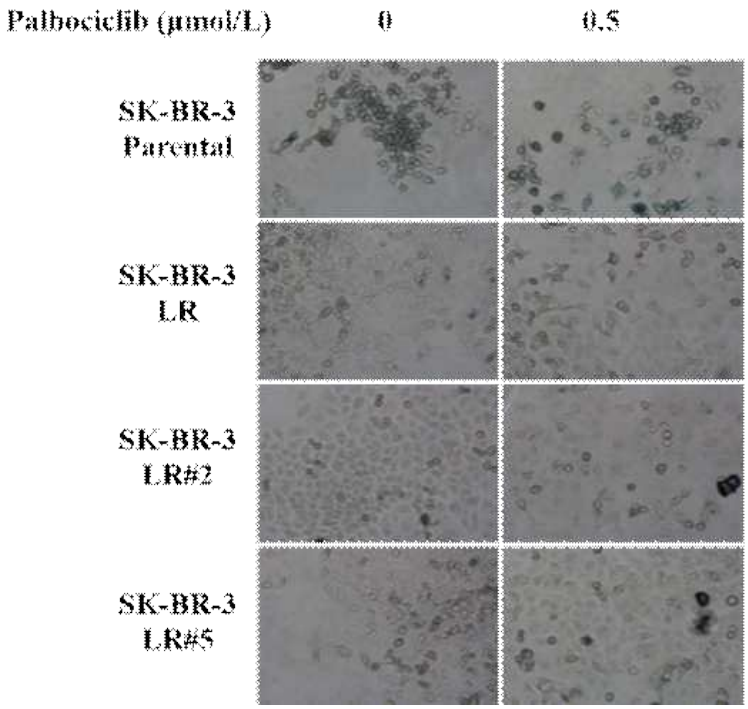

Figure 23. Senescence induction was analyzed by β-galactosidase assay.

Palbociclib was treated 3 times for 120 hours. There was no β-galactosidase staining in SK-BR-3 LR cells.

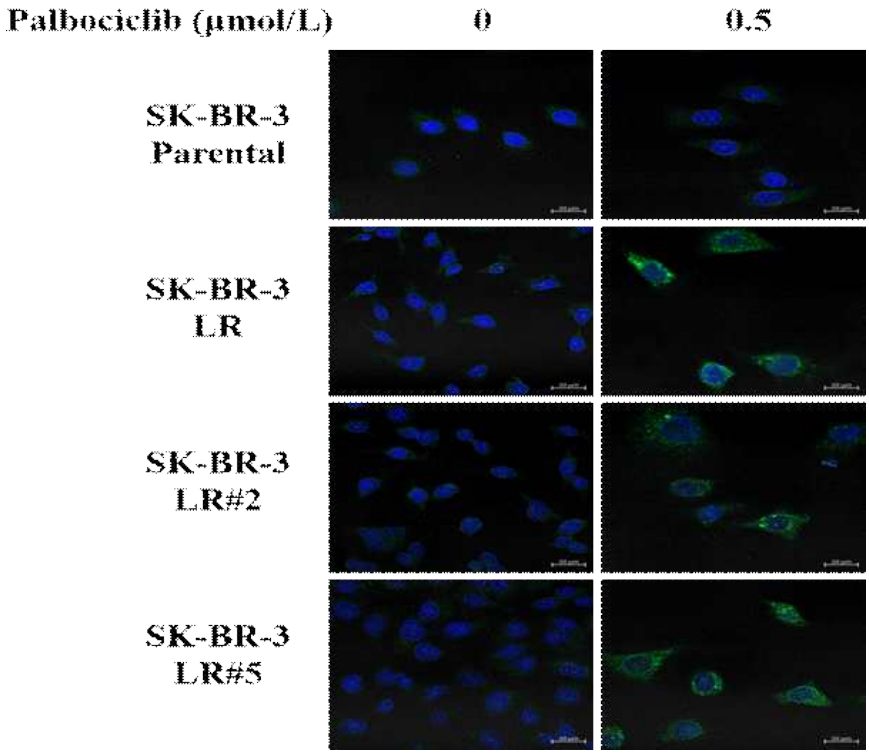

Figure 24. IFA was conducted to determine whether autophagy was induced by palbociclib.

LC3B puncta were detected after palbociclib treatment for 120 hours.

6. Palbociclib was effective in patient-derived xenograft model.

IMX57 PDX model was established from hormone receptor positive and HER2 amplified breast cancer patients who failed many prior lines of HER2 targeted therapies including trastuzumab and lapatinib and endocrine therapy. In this tumor model, the copy number gain of the *CCND1* gene was detected (Fig 25). with upregulation of cyclin D1 protein expression and loss of p14, p16 which were coded by *CDKN2A* (Fig 26). This model is expected to be effective for palbociclib because of the increased G1/S transition due to overactivation of cyclin D1 and *CDKN2A* loss as in SK-BR-3 LR cells. We transplanted PDX sample in mouse at 8 weeks and treated palbociclib (150 mg/kg) daily for 4 weeks. As a result, significant tumor growth was delayed in the palbociclib-treated group (Fig 27). Reduced cell proliferation was observed by decrease of Ki-67 and TS

expression (Fig 28). These results suggest that palbociclib may be an effective treatment strategy for patients with breast cancer who were hyperactivated by cyclin D1 due to loss of *CDKN2A* as they acquired resistance to HER2 targeted therapy.

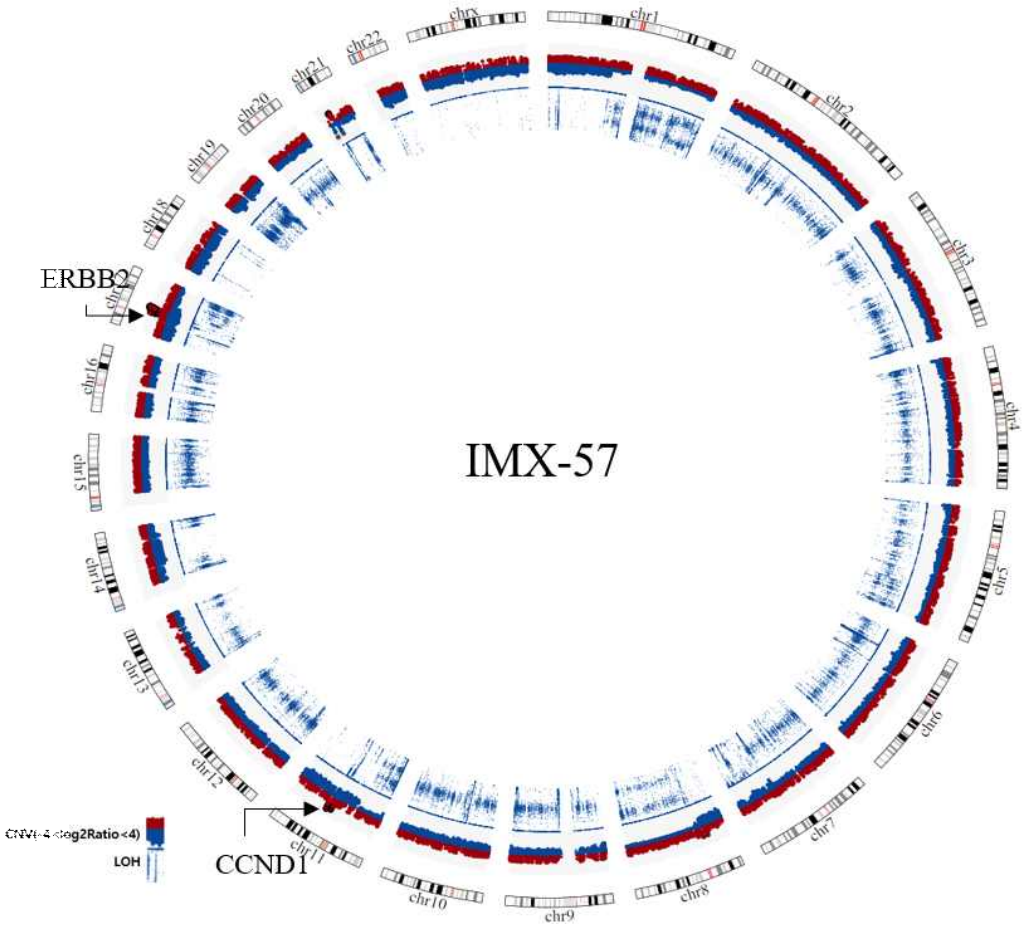

Figure 25. *CCND1* amplification in IMX57 PDX model.

CCND1 and *ERBB2* genes are amplified in IMX57.

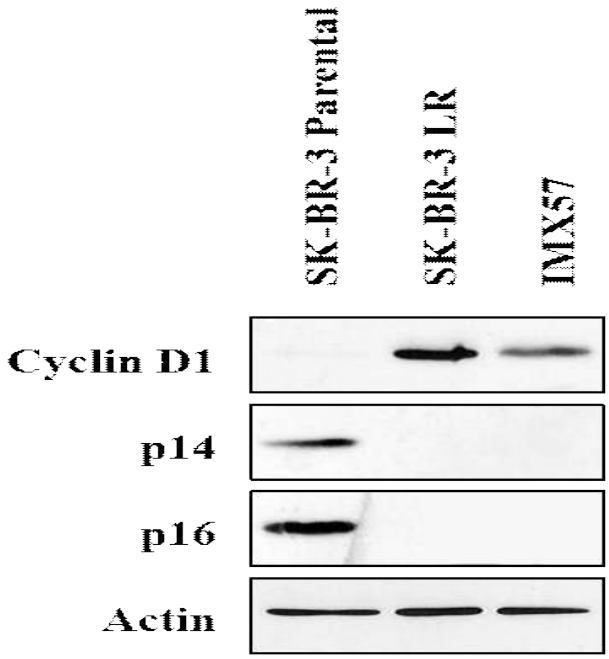

Figure 26. IMX57 have similar characteristics with SK-BR-3 LR cells.

In SK-BR-3 LR cells and IMX57, cyclin D1 was upregulated and *CDKN2A* was downregulated compared to SK-BR-3 parental cells.

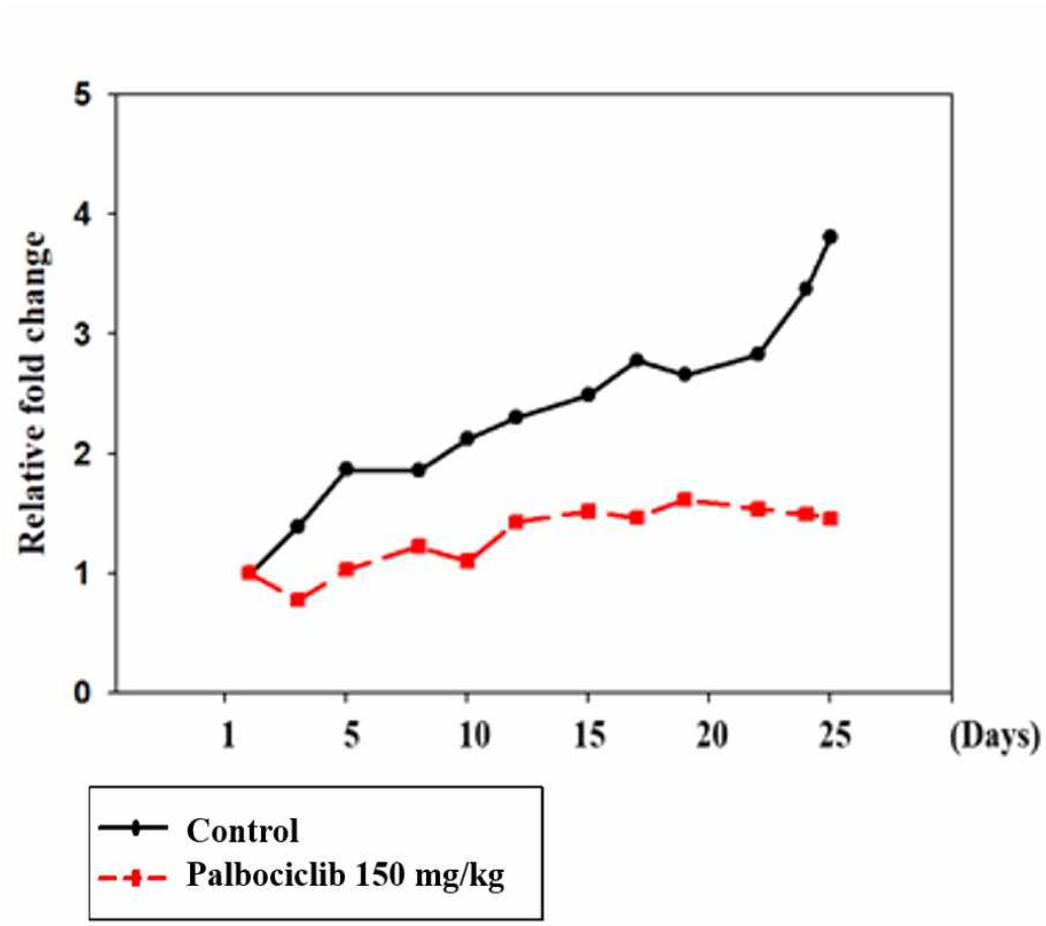

Figure 27. Palbociclib treatment was effective in PDX established from HER2 amplified breast cancer patient failed to lapatinib.

In the vehicle treated group, tumor size was continuously increased, but tumor growth was delayed in palbociclib treated group.

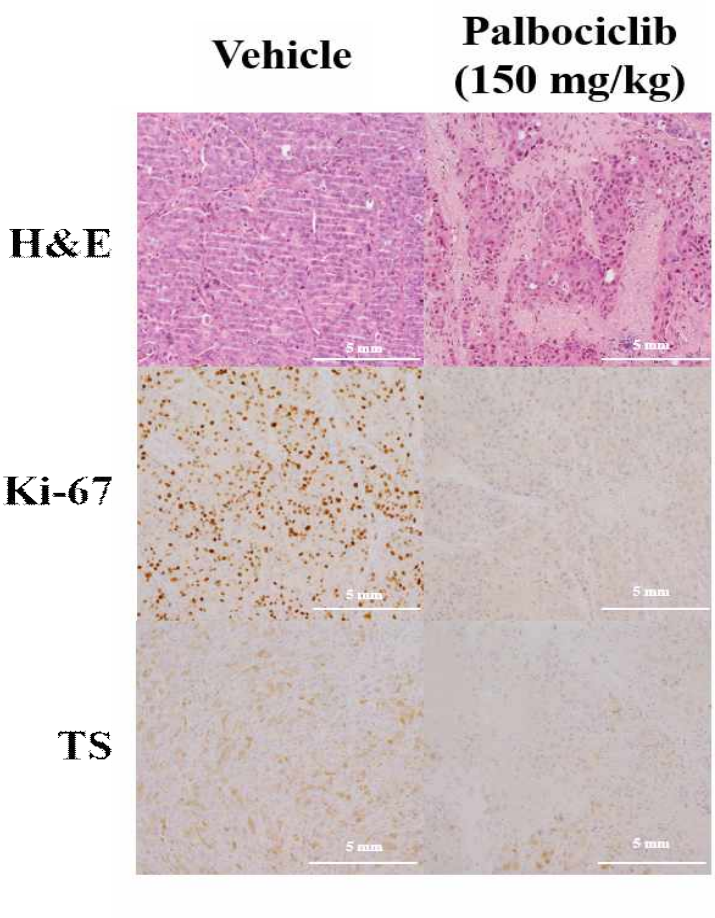

Figure 28. IHC staining of PDX tumor.

Pathological examination was performed using tumor tissue of PDX model after the drug treatment ended. Hematoxylin and eosin (H&E) staining were used and the scale bars represent 5 mm (x10). In the palbociclib treated group, the reduction in TS and Ki-67 expression showed decrease in proliferation.

Discussion

Lapatinib is a HER2 targeted small molecular tyrosine kinase inhibitor that has been effective in HER2 positive breast cancer and gastric cancer [3, 4]. However, due to acquired resistance, there was limitation to use lapatinib for long term treatment [5-7]. Although the mechanism causing this resistance has been actively researched and various drugs have been developed, the overcoming mechanism has not been studied much yet.

In this study, I tried to find a way to overcome the lapatinib resistance and identify its mechanism. For this, lapatinib resistance SK-BR-3 cells were established and their characteritics were analyzed. SK-BR-3 LR cells showed remarkably faster cell proliferation than SK-BR-3 parental cells. But HER2 signaling pathway, which causes proliferation in HER2 positive cells was downregulated [1]. HER2 downstream molecules were first observed

because the altered SK-BR-3 LR cells traits may have been caused by an abnormal increase in proliferation signaling [7, 28-30]. However, the activity of PI3K and MAPK, which are typical HER2 downstream pathways, was decreased. In addition, activity of STAT3, which is another proliferation signal, was increased but it did not affect the viability of SK-BR-3 LR cells. Taken together, these indicate that there might be other mechanism involved in the rapid proliferation of SK-BR-3 LR cells.

By transcriptome data and methylation analysis, it has been found that unlike the SK-BR-3 parental cells, cell cycle-related molecules, especially genes inducing G1/S transition, are upregulated and inhibitors suppressing them are epigenetically inhibited. Previous studies have shown that cell cycle deregulation is one of the mechanisms of lapatinib resistance [8, 9]. The cyclin D-CDK4/6 pathway plays an important role in the transition from G1 to S phase during the cell cycle and is tightly regulated through checkpoint.

However, excessive activation of these pathways is known to induced tumorigenesis [11, 12] and drug resistance. In this regard, the cell cycle progression was also abnormally increased in the SK-BR-3 LR cells, so it could be assumed that inhibition of this pathway would overcome this resistance. Like hypothesis, treatment with palbociclib, which inhibits the cyclin D-CDK4/6 pathway, proved to be more effective in SK-BR-3 LR cells than SK-BR-3 parental cells.

I examined the mechanism of palbociclib in SK-BR-3 LR cells. In short term effect, S phase incorporation was significantly reduced by palbociclib in SK-BR-3 LR cells compared to SK-BR-3 parental cells. Palbociclib was also very effective in the long term culture system, confirmed by CFA. Several previous studies have reported that the effect of palbociclib induced via senescence. Recently, however, palbociclib has been reported to cause autophagy. Palbociclib have shown to induce autophagy and apoptosis in hepatocellular carcinoma (HCC) through the activation of 5'-AMP-activated protein kinase

(AMPK) and the inhibition of protein phosphatase 5 (PP5) [23]. In SK-BR-3 LR cells, it was confirmed that palbociclib induces autophagy. In addition, I confirmed that the antitumor effect of palbociclib was also applied *in vivo* using PDX model established from breast cancer patient with resistance to HER2 targeted therapy that have characteristics of high level of cyclin D1 with *CDKN2A* loss similar to SK-BR-3 LR cells.

In conclusion, palbociclib does not overcome the resistance of lapatinib, but treatment alone is effective enough in SK-BR-3 LR cells. In addition, these results showed that palbociclib can be applied not only to hormone receptor positive breast cancer but also to other subtypes. It was also expected that it would be possible to perform clinical application of palbociclib to HER2 targeted therapy resistant breast cancer by verifying the effect in PDX model.

Reference

[1] Fink MY, Chipuk JE. Survival of HER2-Positive Breast Cancer Cells: Receptor Signaling to Apoptotic Control Centers. Genes Cancer. 2013. 4(5-6):187-9

[2] Jennifer L. Hsu, Mien-Chie Hung. The role of HER2, EGFR, and other receptor tyrosine kinases in breast cancer. Cancer Metastasis Rev. 2016. 35(4):575-588.

[3] Mendes D, Alves C, Afonso N, Cardoso F, Passos-Coelho JL, Costa L, Andrade S, et al. The benefit of HER2-targeted therapies on overall survival of patients with metastatic HER2-positive breast cancer – a systematic review. Breast Cancer Res. 2015. 17:140.

[4] Nelson MH, Dolder CR. Lapatinib: a novel dual tyrosine kinase inhibitor with activity in solid tumors. Ann Pharmacother. 2006. 40(2):261-9.

[5] D'Amato V, Raimondo L, Formisano L, Giuliano M, De Placido S, Rosa R, et al. Mechanisms of lapatinib resistance in HER2-driven breast cancer. Cancer Treat Rev. 2015. 41(10):877-83.

[6] Masoud V, Pagès G. Targeted therapies in breast cancer: New challenges to fight against resistance. World J Clin Oncol. 2017. 8(2):120-134.

[7] Rexer BN, Arteaga CL. Intrinsic and acquired resistance to HER2-targeted therapies in HER2 gene-amplified breast cancer: mechanisms and clinical implications. Crit Rev Oncog. 2012.

17(1):1-16.

[8] Zhuo WL, Zhang L, Xie QC, Zhu B, Chen ZT. Identifying differentially expressed genes and screening small molecule drugs for lapatinib-resistance of breast cancer by a bioinformatics strategy. Asian Pac J Cancer Prev. 2014 15(24):10847-53.

[9] Goel S, Wang Q, Watt AC, Tolaney SM, Dillon DA, Li W, et al. Overcoming Therapeutic Resistance in HER2-Positive Breast Cancers with CDK4/6 Inhibitors. Cancer Cell. 2016. 29(3):255-269.

[10] Kevin J. Barnum, Matthew J. O'Connell. Cell Cycle Regulation by Checkpoints. Methods Mol Biol. 2014. 1170:29 - 40.

[11] Hanahan D, Weinberg RA. Hallmarks of Cancer: The Next Generation. Cell. 2011. 144(5):646-74.

[12] Sherr CJ, Roberts JM. CDK inhibitors: positive and negative regulators of G1-phase progression. Genes Dev. 1999. 13(12):1501-12.

[13] Schedin TB, Borges VF, Shagisultanova E. Overcoming Therapeutic Resistance of Triple Positive Breast Cancer with CDK4/6 Inhibition. Int J Breast Cancer. 2018. 7835095

[14] Scott SC, Lee SS, Abraham J. Mechanisms of therapeutic CDK4/6 inhibition in breast cancer. Semin Oncol. 2017. 44(6):385-394.

[15] Sammons SL, Topping DL, Blackwell KL. HR+, HER2- Advanced Breast Cancer and CDK4/6 Inhibitors: Mode of Action, Clinical Activity, and Safety Profiles. Curr Cancer Drug Targets. 2017. 17(7):637-649.

[16] LaBaer J, Garrett MD, Stevenson LF, Slingerland JM, Sandhu C, Chou HS, et al. New functional activities for the p21 family of CDK

inhibitors. Genes Dev. 1997. 1;11(7):847-62.

[17] Cheng M1, Olivier P, Diehl JA, Fero M, Roussel MF, Roberts JM, et al. The p21(Cip1) and p27(Kip1) CDK 'inhibitors' are essential activators of cyclin D-dependent kinases in murine fibroblasts. EMBO J. 1999. 15;18(6):1571-83.

[18] B Colleoni, S Paternot, JM Pita, X Bisteau, K Coulonval, RJ Davis, et al. JNKs function as CDK4-activating kinases by phosphorylating CDK4 and p21. 2017. 27;36(30)4349-4361.

[19] Diehl JA, Cheng M, Roussel MF, Sherr CJ. Glycogen synthase kinase-3beta regulates cyclin D1 proteolysis and subcellular localization. Genes Dev. 1998. 15;12(22):3499-511.

[20] Alao JP. The regulation of cyclin D1 degradation: roles in cancer development and the potential for therapeutic invention. Mol Cancer. 2007. 2;6:24.

[21] Alt JR, Gladden AB, Diehl JA. p21(Cip1) Promotes cyclin D1 nuclear accumulation via direct inhibition of nuclear export. J Biol Chem. 2002. 8;277(10):8517-23.

[22] Thangavel C, Boopathi E, Liu Y, McNair C, Haber A, Perepelyuk M, et al. Therapeutic Challenge with a CDK 4/6 Inhibitor Induces an RB-Dependent SMAC-Mediated Apoptotic Response in Non-Small Cell Lung Cancer. Clin Cancer Res. 2018. 24(6):1402-1414.

[23] Hsieh FS, Chen YL, Hung MH, Chu PY, Tsai MH, Chen LJ, et al. Palbociclib induces activation of AMPK and inhibits hepatocellular carcinoma in a CDK4/6-independent manner. Mol Oncol. 2017. 11(8):1035-1049.

[24] Akihiro Yoshida, J. Alan Diehl. CDK4/6 inhibitor: from quiescence to senescence. Oncoscience 2015. 2(11):896 - 897.

[25] Valenzuela CA, Vargas L, Martinez V, Bravo S, Brown NE. Palbociclib-induced autophagy and senescence in gastric cancer cells. Exp Cell Res 2017. 360(2):390-396.

[26] Klein ME, Dickson MA, Antonescu C, Qin LX, Dooley SJ, Barlas A, et al. PDLIM7 and CDH18 regulate the turnover of MDM2 during CDK4/6 inhibitor therapy-induced senescence. Oncogene. 2018. 37(37):5066-5078.

[27] Stephanie H. Scott, Brian J. Bahnson. Senescence Marker Protein 30: Functional and Structural Insights to its Unknown Physiological Function. Biomol Concepts. 2011. 2(6):469 - 480.

[28] Natalia J. Sumi, Brent M. Kuenzi, Claire E. Knezevic, Lily L. Remsing Rix, et al. Chemoproteomics reveals novel protein and lipid kinase targets of clinical CDK4/6 inhibitors in lung cancer. ACS Chem Biol. 2015. 10(12):2680 - 2686.

[29] Kirouac DC, Du J, Lahdenranta J, Onsum MD, Nielsen UB, Schoeberl B, et al. HER2+ Cancer Cell Dependence on PI3K vs. MAPK Signaling Axes Is Determined by Expression of EGFR, ERBB3 and CDKN1B. PLoS Comput Biol. 2016. 12(4):e1004827.

[30] Chung SS, Giehl N, Wu Y, Vadgama JV. STAT3 activation in HER2-overexpressing breast cancer promotes epithelial-mesenchymal transition and cancer stem cell traits. Int J Oncol. 2014. 44(2):403-11

국문 초록

Lapatinib은 HER2와 epidermal growth factor receptor (EGFR)을 차단하는 이중 tyrosine kinase 억제제로써 HER2 양성 전이성 유방암에서 효과적으로 작용하나 치료 중 내성이 나타난다. Cyclin D-CDK4/6 복합체의 과도한 활성으로 인한 무분별한 세포주기 활성은 lapatinib에 대한 획득 내성 기전으로 알려져 있다. 따라서 lapatinib 내성을 극복하기 위한 전략으로 cyclin D-CDK4/6 경로를 활용할 수 있을 것으로 판단하였다. 본 연구에서는 CDK4/6 억제제인 palbociclib이 세포주기를 조절하여 lapatinib 내성 세포에서 항종양효과를 나타내는지 확인하고, 그 기전을 연구하여 lapatinib 내성 HER2 양성 유방암의 새로운 치료 전략으로 사용될 수 있는지 연구하였다.

HER2 양성 유방암 세포주 SK-BR-3에 lapatinib의 농도를 증가시키면서 장기간 처리하여 내성이 생긴 세포주를 수립하고 transcriptome data, FACS, Western blotting, qPCR, methylation assay 등을 통해 lapatinib 내성 세포주의 특성을 확인하였다. MTT, BrdU assay와 콜로니 형성 분석의 변화를 통해 palbociclib의 세포 증식억제 효과를 관찰하였고, 세포

주기에 관여하는 분자와 신호 전달경로에 관여하는 분자들의 발현 변화 및 β-galactosidase assay와 IFA를 통해 기전을 연구하였다.

Lapatinib 내성 세포에서는 세포주기의 G1/S 이행과 관련된 분자들의 변화가 두드러지게 나타났으며 SK-BR-3 부모 세포와 비교하여 세포주기의 진행과 증식 속도가 증가되어 있었다. 이와 관련하여 lapatinib에 대한 내성 기전 중 하나인 cyclin D-CDK4/6 복합체의 활성이 증가하고 이들을 억제하는 CKI인 *CDKN2A*가 메틸화로 인해 억제되어 있었다. Cyclin D1과 CDK6 발현은 전사수준에서 증가 되었고 *CDKN2A*는 후성유전 억제나 이 결과를 통해 *CDKN2A*의 억제로 인해 cyclin D1의 활성화가 유발되었다고 판단하였다. Palbociclib은 Rb의 인산화를 억제하여 lapatinib 내성 HER2 양성 유방암 세포주에서 세포주기 진행을 억제하고 세포 생존 능력을 현저하게 감소시킨다는 것을 확인하였으며 palbociclib이 lapatinib 내성 세포에서 자가소화작용을 유발하여 세포성장 억제 효과를 나타낸다는 것을 확인하였다. HER2 표적 치료제에 내성이 생겨 *CDKN2A*의 억제와 cyclin D1의 증가가 일어난 HER2 양성 유방암 환자로부터 얻은 환자유래 종양 동물 모델에서도 palbociclib이 효과적으로

종양의 성장을 억제함을 확인하였다.

따라서 palbociclib에 의한 세포 주기 경로의 억제는 lapatinib 내성 HER2 양성 유방암 치료에 효과적인 전략이 될 수 있으며 본 연구 결과를 통해 palbociclib이 호르몬 수용체 양성 유방암뿐만 아니라 다른 아형에서도 적용이 가능하다는 것을 보여주었고 환자유래 종양 동물 모델에서 검증하여 빠른 임상 적용을 할 수 있을 것이라 기대할 수 있다.

주요어 : HER2, lapatinib, 내성, 세포주기, CDK4/6 억제제, 자가소화작용, 환자유래 종양 동물 모델

학번 : 2017-26288

Acknowledgement

GSK and Pfizer kindly provided lapatinib and palbociclib through MTA contract with professor Seock-Ah Im, Kyung-Hun Lee, and Ahrum Min. This study was carried out through the idea and funding source of Seock-Ah Im, and was supported by So Hyeon Kim, Seongyeong Kim, Yu-Jin Kim, YoonJung Park.